CORTICAL CONSEQUENCES OF ELEVATED INTRAOCULAR PRESSURE IN A PRIMATE MODEL OF GLAUCOMA

by

DAWN YUEN SIC LAM

B.Sc., THE UNVERSITY OF BRITISH COLUMBIA, 1989

A THESIS SUBMITTED IN PARTIAL FULFILMENT OF THE REQUIREMENTS FOR THE DEGREE OF

MASTER OF SCIENCE

IN

THE FACULTY OF GRADUATE STUDIES

(Graduate Program in Neuroscience)

We accept this thesis as conforming to the required standard

THE UNIVERSITY OF BRITISH COLUMBIA

July 2001

In presenting this thesis in partial fulfilment of the requirements for an advanced degree at the University of British Columbia, I agree that the Library shall make it freely available for reference and study. I further agree that permission for extensive copying of this thesis for scholarly purposes may be granted by the head of my department or by his or her representatives. It is understood that copying or publication of this thesis for financial gain shall not be allowed without my written permission.

Graduate Program in Neuroscience

Department of ~~Department of~~ Ophthalmology

The University of British Columbia
Vancouver, Canada

Date Aug 9, 2001

Abstract

Glaucoma is a disease which affects the optic nerve. Its effects lead to debilitating visual deficits and there are no known cures. The primate model of glaucoma was developed so that investigators can study this disease. Research in glaucoma has examined the disease at the level of the eye and at the level of the lateral geniculate nucleus; however, few have looked at the consequence of this disease at the level of the visual cortex. This study looks at the effects of elevated intraocular pressure (IOP) over a period of seven months by examining the density of metabolic activity markers and neurochemical markers in primary visual cortex.

Elevated IOP was induced by unilaterally lasering the trabecular meshwork of primates. Elevated IOP was monitored periodically over a period of two to seven months before the animals were sacrificed and the cortex processed histochemically for cytochrome oxidase (CO) and immunohistochemically for growth-associated protein 43 (GAP-43), synaptophysin (SYN), γ-aminobutyric acid receptor (GABAa receptor) and calcium-dependent protein kinase II α (CAMKIIα).

CO density was found to be lower in deprived eye columns than in non-deprived eye columns suggesting that there was a decrease in metabolic activity in the eye subjected to elevated IOP. GAP-43, SYN and GABAa receptor densities were found to be greater in non-deprived eye columns than in deprived eye columns. In contrast, CAMKIIα protein densities were found to be greater in deprived eye columns than in non-deprived eye columns. When comparing the optical densities in the visual cortex of experimental animals to normal animals, the protein densities of GAP-43 and SYN were found to be higher in the experimental animals than in the normal animals. The protein densities of GABAa receptor and CAMKIIα were found to be lower in experimental animals than in normal animals.

Our results suggest that elevated IOP caused cortical changes as early as two months post-elevated IOP. These changes continued through to seven months post-elevated IOP.

Table of Contents

List of Tables and Figures

List of Abbreviations

IOP-Intraocular Pressure
M - Magnocellular pathway
P - Parvocellular pathway
K - Koniocellular pathway
LGN – lateral geniculate nucleus
CO – cytochrome oxidase
TTX – tetrodotoxin
GAP-43 – growth-associated protein 43
SYN – synaptophysin
GABAa receptor – γ-aminobutyric acid a receptor β2/3 subunit
GAD – glutamic acid decarboxylase
CAMKIIα – type II calcium/calmodulin-dependent protein kinase α subunit
OD – optical density

Acknowledgements

I could not have written this manuscript without the advice and support from Joanne A. Matsubara, Ph.D. I am also grateful for technical and moral support from Eleanor To who helped me whenever things were stressful. I also want to take this time to thank, Virginia Booth, Jing Cui, Tara Stewart, Christian Wong and all others who had a hand in helping me complete this manuscript.

General Introduction

Glaucoma is often referred to as the "sneak thief of sight" because it causes no symptoms until vision is already lost. Glaucoma describes a group of diseases that leads to irreversible damage to the optic nerve and eventual visual loss. Most, but not all of these diseases are characterized by elevated intraocular pressure (IOP) and it is a concern to most clinicians because it is one of the leading causes of blindness in the world. This year it is estimated that 6.7 million people will be blind as a result of glaucoma (Quigley 1996).

Earlier studies have focused on understanding this disease at the level of the eye. The damage to the optic nerve head and the degeneration of retinal ganglion cells make this an obvious area of research; however, full implications of this disease on the central nervous system (CNS) are still largely unknown. Examining the effects of elevated IOP in the adult cortex would be an important step to fully understand the implications of this disease. The purpose of this study is to understand the cortical consequences of elevated IOP. We wish to determine whether there are temporal and spatial changes in neurochemical levels in a primate model of glaucoma. Because there is no cure for this disease and because there is no agreed upon diagnostic tool, researchers are working to understand the consequence of this disease on the entire visual system.

A. Definition of Glaucoma

Glaucoma is a group of diseases defined by damage to the optic disc. It is often characterized by elevated IOP which leads to retinal ganglion cell degeneration and eventual visual loss. Patients afflicted with this disease, both in the presence or absence of elevated IOP, will demonstrate optic disc damage; therefore, both the damage to the retinal ganglion cell layer and the damage to the optic disc are hallmarks of this disease.

To understand the different types of glaucoma, one must first understand IOP. IOP is the "the rate at which aqueous humor enters the eye (inflow) and the rate at which it leaves the eye (outflow)" (Shields M 1992). Inflow depends on the rate of aqueous humor production and outflow depends on the flow of aqueous humor from the eye via the trabecular meshwork. The trabecular meshwork is a structure which consists of the Schlemm's canal, intrascleral channels and episcleral and conjunctival veins (Figure 1) and it is important to understand this structure because many ocular problems associated with glaucoma involve the trabecular meshwork. Normal IOP in a general population with no known eye disease is cited to be 15.5 ± 2.57 mm Hg (Armly 1968; Johnson 1966, Perkins 1965, Segal and Skwiercynska 1967). Increases in IOP can be influenced by factors such as genetics, age, sex, refractive error and race (Armaly 1967, Armaly et al 1968, David et al 1985, Hiller et al 1982, Klein and Klein 1981, Tomlinson and Philips 1970).

Glaucoma can be classified into primary and secondary forms. Glaucoma, which is caused by outflow obstruction and intraocular pressure elevation not related to other ocular or systemic disorders, is classified as primary glaucoma. These include open-angle, closed-angle and congential glaucoma, all of which are confined to the anterior chamber. Secondary glaucoma is usually acquired due to ocular or systemic disorders not related to glaucoma. This type of glaucoma can include congenital, open-angle or closed-angle glaucoma as well. There are four types of glaucoma, each of which are detailed in the appendix.

B. Primate model of glaucoma:

An experimental model of glaucoma is useful to study the effects of elevated intraocular pressure (IOP) on the central visual pathways. The monkey eye is an ideal model for glaucoma because of its similarity to the human eye. This model has helped in determining the pathophysiology of the disease (Dreyer et al 1996; Quigley et al 1995; Varma et al 1992). It

Figure 1 : Open Angle Glaucoma. The: arrow demonstrate the flow of aqueous humour through the anterior chamber of the eye. In open angle glaucoma the aqueous is not draining out of the anterior chamber via trabecular meshwork because the trabecular meshwork is blocked.

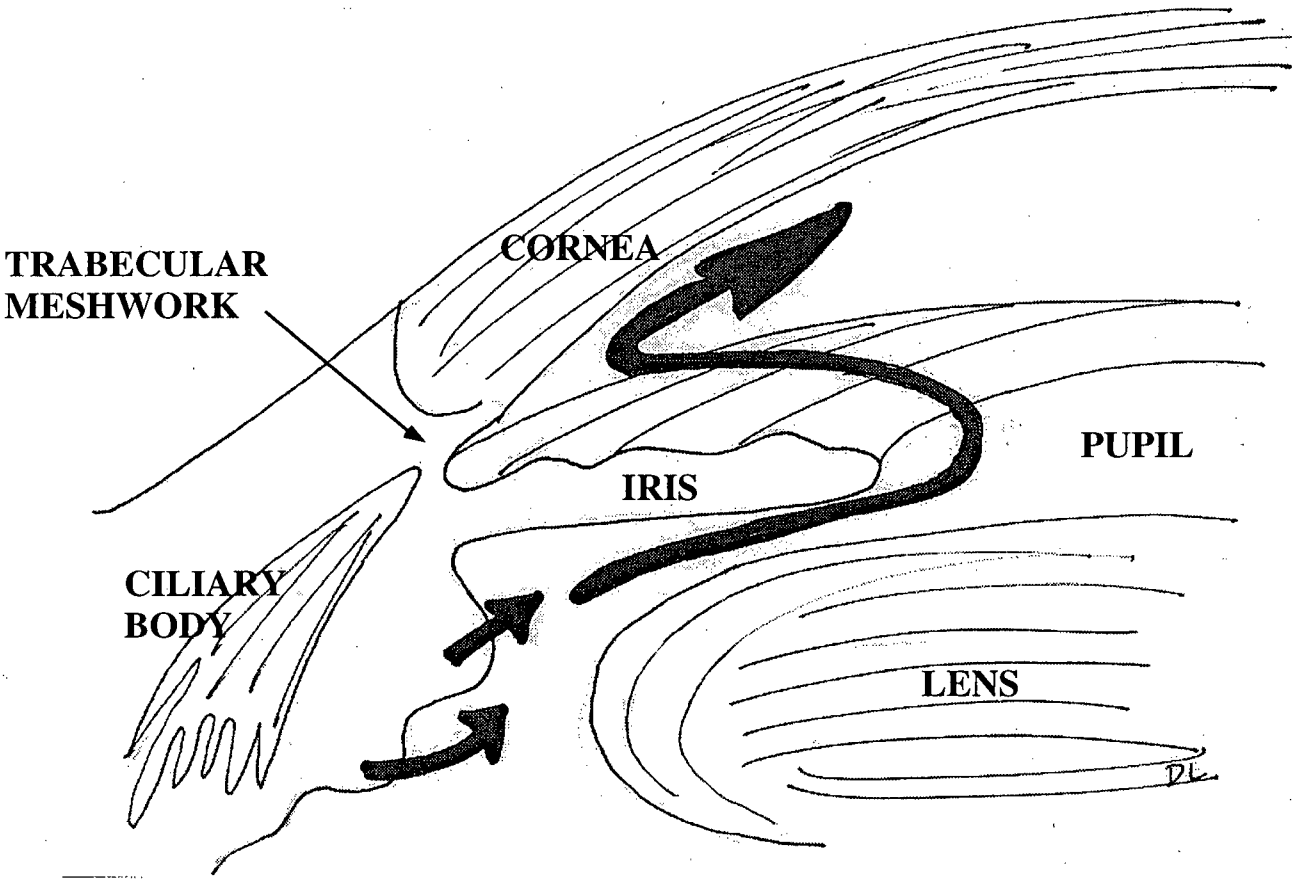
TRABECULAR
MESHWORK
CORNEA
PUPIL
IRIS
CILIARY
BODY
LENS

allows the investigator to examine the effects of elevated IOP over a complete time period from early to end stage glaucoma.

The monkey model of glaucoma, first proposed by Gaasterland and Kupfer (1974), demonstrates a method to provide sustained elevated IOP in the rhesus monkey. An argon laser is used to laser the trabecular meshwork, a structure which is important in facilitating aqueous humor to drain out of the eye. Because the trabecular meshwork is blocked post-lasering, this leads to elevated IOP. The IOP elevation was found to be sufficient to cause selective damage to the retinal ganglion cells and it mimics the damage found in open angle glaucoma (description please see appendix).

This technique allows the investigator to produce a sustained elevated IOP with minimal ocular inflammation. As well, this technique causes cupping of the optic nerve head, blockage of fast axonal transport (Dandona et al 1991), changes in the nerve fiber layer (Quigley and Pease 1996, Yucel et al 1998) and optic nerve characteristic changes (Varma et al 1992) in the primate, all of which are characteristics found in human open-angle glaucoma. Because the most common cause of glaucoma occurs in adult patients, this model in the adult primate allows a study of the effects of elevated IOP in the primary visual cortex.

C. Central Visual Pathway

i. Visual neuroanatomy

When light enters through the pupil of the eye it is focused through the lens and onto the retina at the back of the eye. The retina is composed of 10 layers; the internal limiting membrane, the retinal ganglion cell layer, the inner plexiform layer, the inner nuclear layer, the outer plexiform layer, the outer nuclear layer, the inner photoreceptor segment, the outer photoreceptor segment, the retinal pigment epithelium and the choroid. The cells in the retina transform the light signal into a chemical signal which leaves the eye via the optic nerve. The photoreceptor

layer is the first retinal layer to transduce the light signal to a chemical signal which then passes through the other layers to the retinal ganglion cells. The axons of the retinal ganglion cells travel through the nerve fiber layer to the optic disc head where it becomes bundles of axons which leave the eye.

The axons from the optic nerve project to the dorsal LGN; however, before reaching the LGN, some of the axons within the optic nerve cross at the optic chiasm. Axons of retinal ganglion cells from nasal retina cross over at the optic chiasm to the other hemisphere and continue to the contralateral LGN. Axons of the retinal ganglion cells of the temporal retina remain uncrossed and terminate in the ipsilateral LGN (Figure 2). From there, the visual information travels to the visual cortex and terminates in layer 4C (Figure 2). This results in each hemisphere of the brain receiving information from the opposite the visual field i.e. the right hemisphere receives information from the left visual field and vice versa for the left hemisphere.

The LGN is a bilateral thalamic structure. It has a total of 6 principal layers. Layers 1, 4 and 6 receive visual input from the contralateral eye and layers 2, 3 and 5 receives visual input from the ipsilateral eye. Despite the separate inputs from the two eyes into different layers, the topographical arrangement of ganglion receptive fields are conserved in each layer of the LGN; therefore, consequences of monocular retinal damage by elevated IOP can also be evaluated at the level of the LGN.

The primary visual cortex (area V1) receives the strongest input from the LGN, but it also receives input from other thalamic nuclei, such as the medial interlaminar nucleus and the lateral posterior/pulvinar complex (Benevento and Rezak 1976). Area V1 receives visual signals via parallel pathways from the thalamus and is the source of output to higher-order visual areas (Casagrande and Kaas 1994). In area V1, the cells are organized into columns which have

Figure 2: Visual Pathway. Visual information processed in the temporal retina travels down the optic tract and continues to the ipsilateral lateral geniculate nucleus (LGN). Retinogeniculo-afferents synapse in layers 2, 3 and 5 of the LGN. Visual information processed in the nasal retina travels down the optic tract and continues to the contralateral LGN where it synapses with layers 1, 4 and 6 of the LGN. Geniculocortical afferents from layers 1 and 2 of the LGN belong to the magnocellular pathway (M) and afferents from layers 3, 4, 5 and 6 belong to the parvocellular pathway (P). Both these pathways remain segregated as they travel to the visual cortex.

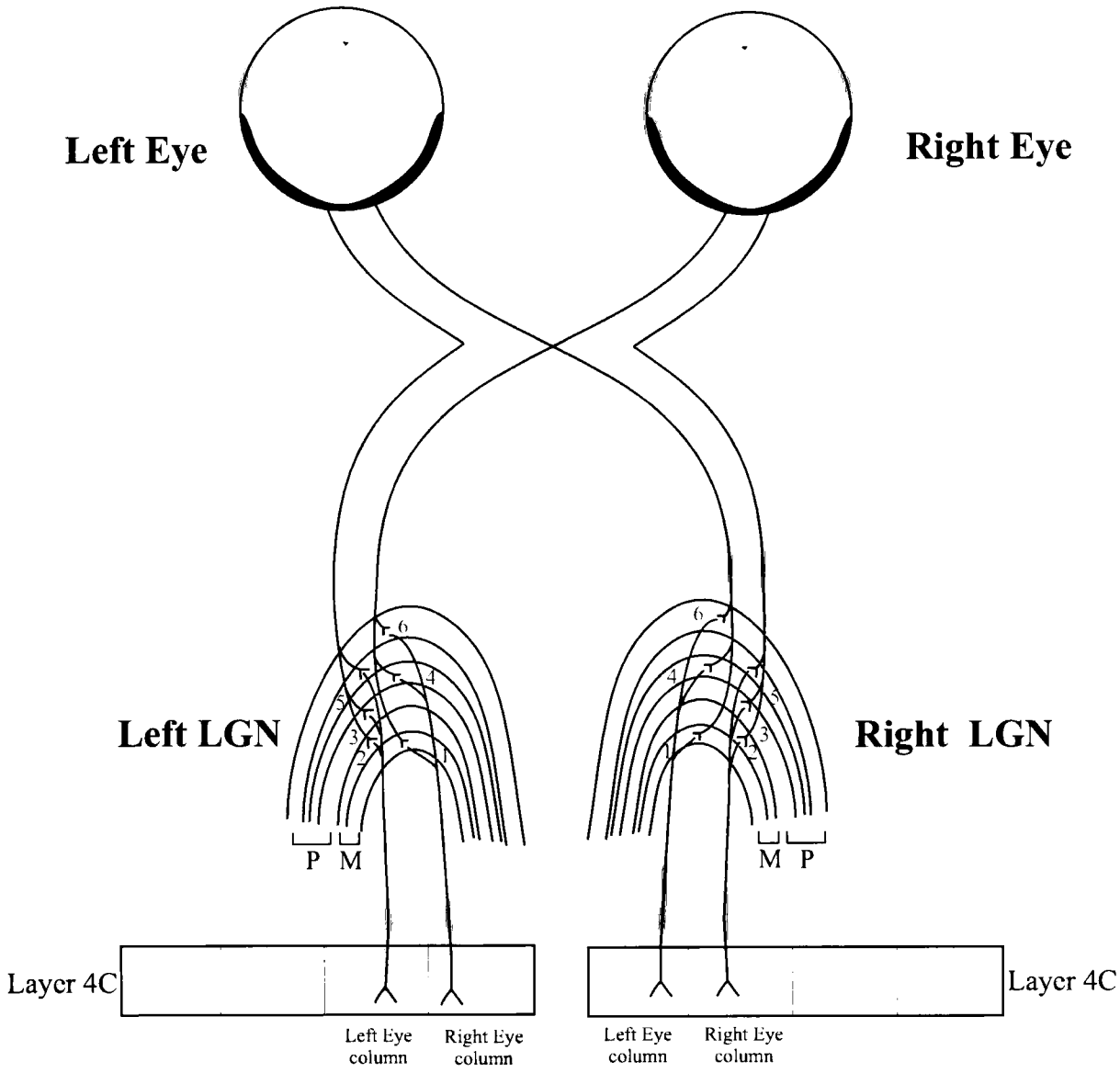
Left Eye
Right Eye
Left LGN
Right LGN
6
5
4
3
2
1
P
M
M
P
Layer 4C
Layer 4C
Left Eye column
Right Eye column
Left Eye column
Right Eye column
Left Visual Cortex
Right Visual Cortex

similar orientation and directional properties and are eye specific. The geniculocortical layer, layer 4, is subdivided into 3 sublayers, 4A, 4B and 4C. Sublayer 4C is further subdivided into layer 4Cα and 4Cβ. From layer 4C, intracortical projections are made to layers 2/3 and 5/6. Projections are then made out of layers 2/3 to higher cortical regions such as area V2. Layer 5/6 projects mainly to subcortical areas i.e. superior colliculus and LGN. For our purposes, we are interested in observing the effects of elevated IOP on the geniculocortical layer.

Although the retinogeniculocortical pathway is the primary visual pathway; the retina does also projects to the superior colliculus, the pulvinar nucleus, the pregeniculate nucleus, the olivary pretectal nucleus, the nucleus optic tract, the dorsal, the lateral and the medial terminal accessory optic nucleus and the suprachiasmatic nucleus (Cowey and Stoerig 1993). These pathways are responsible for driving ocular motility, circadian rhythms, and governing pupillary light reflex.

ii. Parallel Processing Streams

Studies on the primate model and in glaucomatous patients have suggested that there is preferential loss of one or more of the parallel processing streams (Quigley et al 1988; Weber et al 2000; Yucel et al 2000). At the level of the retina, the visual system can be divided into three separate, but parallel processing pathways. The retina consists of three different retinal ganglion cell types. Aapproximately 80% are parvocellular type ganglion cells, 10% are magnocellular type ganglion cells and the last 10% are Koniocellular type ganglion cells. These pathways remain separate, but parallel as they travel via the optic nerve to the visual cortex.

Layers 1 and 2 of the LGN receive information from the magnocellular pathway (M-pathway) and layers 3, 4, 5, and 6 receive information from the parvocellular pathway (P-pathway). The koniocellular pathway (K pathway) terminates in the interlaminar layers of the LGN. The P, the M and the K cells in the LGN then project and terminate at distinct targets in

the visual cortex. The P pathway is generally associated with perception of colour and form (Livingstone and Hubel 1988) and is sensitive to chromatic contrast and high spatial resolution. The M pathway is generally associated with perception of motion and high temporal resolution (Casagrande and Kaas 1994). The characteristics of the K pathway are least well known, but it has been hypothesized to be involved in colour vision. Amongst these three pathways it has been suggested that there may be an early preferential M-pathway loss in glaucomatous patients. Because this pathway is associated with motion perception it suggests a possible diagnostic tool for clinicians to use to screen for early glaucomatous damage in patients.

In the striate cortex, the CO blobs and interblobs have different physiological properties with respect to the layers associated with the P and M pathways (Livingstone and Hubel 1988, 1987). The P-pathway terminates in layers 4A and 4Cβ and the M-pathway terminates in layers 4Cα (Hendrickson et al 1978; Hubel and Wiesel 1972). Neurons from 4Cβ project to layers 2 and 3 and neurons in 4Cα projects up to layer 4B. From layer 2/3 and 4B projections are then sent to extrastriate areas V2, V3, V4 and V5 (area MT). Recently a few investigators have examined area V1 for a preferential M-pathway loss in experimental glaucoma (Crawford et al 2000; Vickers et al 1997); however, no one has examined the effects of elevated IOP on the extrastriate regions associated with the M-pathway (area MT).

The third parallel pathway (K) is least well known; however, it was found via anatomical studies to be located in the interlaminar and superficial (S) layers of the LGN (Hendry and Yoshioka 1994; Livingstone and Hubel 1982). Koniocellular LGN axons project to the CO blobs in layer III whereas magnocellular and parvocellular LGN cells terminate in the upper and lower divisions of layer 4 respectively. The K pathway is distinct in that it stains densely for calbindin, and lightly for CO and parvalbumin (Johnson and Casagrande 1993). The M and the P layers on the other hand stains lightly for calbindin, and densely for cytochrome oxidase (CO) and

parvalbumin (Johnson and Casagrande 1993). One novel marker that emerged to stain for the LGN axons of the K pathway was calcium/calmodulin dependent protein kinase IIα (CAMKIIα) (Hendry and Yoshioka 1994); however, the relationship between this marker and the K-pathway is still unknown.

iii. Topography

In glaucomatous primates and patients, it is found that elevated IOP causes damage to the optic nerve in topographic register to visual field damage. Similar to the LGN, the visual field is also topographically organized throughout the visual cortex with greater cortical areas devoted to central vision (Polyak 1957). Knowledge of visual field representations in the cortex allows investigators to determine what, if any, transformation take place after visual manipulations; however, because more than half of the striate cortex is located within the calcarine sulcus, techniques were developed to map out the regions in the sulcus. Two-dimensional representations of the cortical surface in conjunction with physiological recordings were previously used to demonstrate the visual fields over the entire surface of striate cortex (Daniel and Whitteridge 1961). Van Essen and Maunsell (1980) later developed the technique of using outlines of histological sections to construct accurate two-dimensional representations of the visual cortex.

The striate cortex, if flattened as described by Horton and Hocking (1996) (Figure 3) can demonstrate major geographical features (Figure 3). The operculum of the visual cortex is itself fairly flat and smooth; however, because part of the visual cortex is located within the calcarine sulcus and along the calcarine fissure (Kennedy et al 1975; LeVay et al 1980; LeVay et al 1985; Van Essen et al 1984) these areas can be divided into four cortical blocks. A 'hinge' area (Horton and Hocking 1996) separates the operculum surface from the calcarine blocks which

Figure 3: Flattened Primary Visual Cortex. A flattened representation of the primary visual cortex showing blocks 1, 2, 3 and 4. Dotted lines represent the borders of each block. This figure is adapted from Horton and Hubel 1996. Block 1 (Operculum) represents the central visual field representation. The calcarine sulcus separates block 1 from blocks 3 and 4; therefore, after flattening, blocks 2, 3 and 4 are flattened and they represent the roof of the calcarine sulcus, the ventral bank of the sulcus and the dorsal bank of the sulcus represent the peripheral visual field representation. Cortex representing the central 8-10 degrees of vision is lost during the flattening procedure.

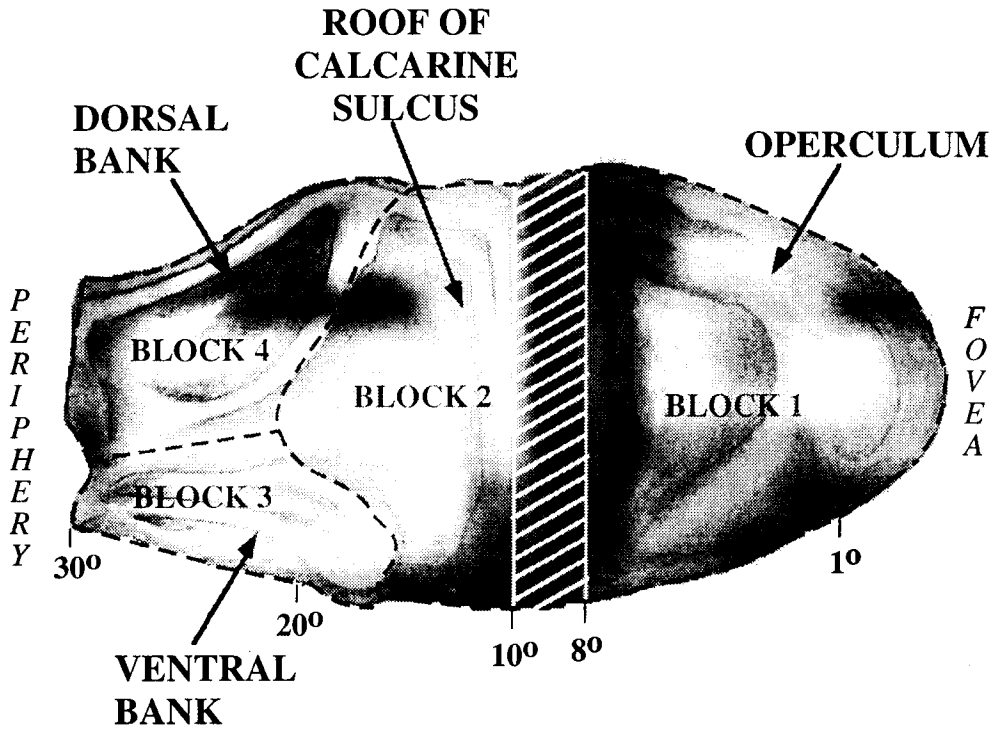
ROOF OF
CALCARINE
SULCUS
DORSAL
BANK
OPERCULUM
PERIPHERY
FOVEA
BLOCK 4
BLOCK 2
BLOCK 1
BLOCK 3
30°
20°
10°
8°
1°
VENTRAL
BANK

consists of the 'roof' of the calcarine sulcus (Figure 3), the dorsal bank and the ventral bank of the calcarine fissure (Figure 3).

D. Effects of elevated IOP on the Visual Pathway

The primate model allows the investigator to examine elevated IOP damage at the level of the retina, the LGN and the visual cortex. The anatomical damage found in glaucoma patients and glaucomatous monkeys (monkeys with elevated IOP) has been found to be quite similar (Dreyer et al 1996; Nickells 1996; Quigley et al 1995; Schumer and Podos 1994). Chronic experimental monkey glaucoma mimics human glaucoma in its physical optic disc changes and in the pattern of ganglion cell loss (Quigley and Addicks 1980, Quilgey et al 1984, 1987).

i. Optic Nerve Head

The optic nerve head (optic disc) is located at the back of the eye, in the most distal portion of the optic nerve. Ganglion cells send their axons via the nerve fiber layer, to the lamina cribosa where it converges and bends into the optic disc. The lamina cribosa consists of sheets of connective tissues and elastic fibers which provides collagen support for the disc. The nerve fiber layer consists of axons from all areas of the retina. Axons from the macula and from the nasal retina terminate in the central portion of the optic nerve. Fibers from the temporal periphery of the retina terminate in the superotemporal and inferotemporal aspects of the optic nerve and it is these fibers which are most susceptible to glaucomatous damage (Minckler 1980; Radius and Anderson 1979;). The central portion of the optic disc contains a depression called the optic cup which tends to enlarge when subjected to glaucomatous damage. Surrounding the outer edge of the cup and the outer margin of the disc is tissue called the neural rim.

Changes in optic disc patterns and nerve fiber layer characterizes glaucomatous optic disc atrophy. The mechanical pressure on the lamina cribosa and possible optic nerve head ischemia (Morgan 2000) causes the neural rim of the optic disc to thin as bundles of axons atrophy in the

inferotemporal and superotemporal areas of the optic disc (Jonas 1993; Jonas et al 1988; Radius et al 1978; Shin et al 1992,). The cup deepens or enlarges (Chandler and Grant 1977; Portney 1976,) and because the optic nerve can be observed clinically, identifying characteristic changes in the optic nerve head is important in the diagnosis of the disease.

Visible defects can be seen in the retinal nerve fiber layer as a result of glaucomatous atrophy. In glaucomatous patients the physiological loss, as measured by visual field testing, is correlated with the loss of axons in the optic nerve (Quigley and Addicks 1981). These are the axons from the midperipheral retina which terminate in the superior and inferior parts of the lamina cribosa of the optic disc. (Minckler 1980; Radius and Anderson 1979).

As the cup enlarges the connective tissues, such as the lamina cribosa, becomes distorted and the fenestrations in the lamina cribosa change shape (Emery et al 1974; Hayreh 1974; Radius 1987). Further, the distortion in the connective tissues causes a backward bowing of the lamina towards the posterior of the optic nerve head (Levy and Crapps 1984; Radius and Pederson 1984; Yan et al 1994,)

ii. Retinal ganglion cell

Ganglion cells from all parts of the retina send their axons along the nerve fiber layer to the optic nerve head. Axons from the macula and nasal retina follow a straight course to the optic nerve head whereas axons from the temporal retina follow an arcuate (a bow-like) path around the macula bundle of axons to reach the optic nerve head. Temporal retinal axons do not cross the horizontal raphe that extends from the fovea to the temporal retinal periphery and they form the boundary between the superior and inferior halves of the retina. Consequently, the arcuate nerve fibers occupy the superior and inferior temporal portions of the optic nerve head with axons from the peripheral retina taking a more peripheral position in the optic nerve. In chronic human glaucoma, the superior and inferior parts of the optic nerve demonstrate greater

atrophy than the nasal and temporal regions (Quigley et al 1982; Quigley et al 1988). In monkeys the loss of retinal ganglion cells is also found to occur in both the midperiphery and the foveal area of the retina (Glovinsky et al 1991, Glovinsky et al 1993, Quigley et al 1989).

Loss of retinal ganglion cells and their axons have been demonstrated histologically in humans with chronic glaucoma and in monkeys with chronic experimental glaucoma (Glovinsky et al 1991; Quigley et al 1987; 1988; 1989, Radius and Pederson et al 1984). Early axonal damage, in humans (Quigley et al 1987) and monkeys (Quigley et al 1987) appear to affect a greater proportion of the larger diameter nerve fibers (fibers presumably of the M-pathway). This is speculated to be due to the fact that the axons in the inferior and superior poles have a greater portion of larger than normal nerve fibers (Quigley et al 1987, 1988). Some studies have reported that large optic nerve fibers and large ganglion cells (M-pathway) are most affected by glaucomatous damage (Glovinsky et al 1991; 1993; Quigley et al 1987; 1988); however, other reports suggest that the magnitude of any differential change between the M- and P- pathway cells are very small (Weber et al 1998). As well, Weber et al (1998) reported that there was a reduction in cell size before degeneration. Previous studies inferring a selective loss in large diameter fibers could be due to this phenomenon.

Axonal loss occurs early in the disease process and is correlated with the size of the optic cup (Gaasterland et al 1978; Quigley and Addicks 1980; Quigley and Green 1979; Radius and Pederson 1984; Varma et al 1992). When the cup/disc ratio exceeds 0.6, there have been reports of glaucoma-related abnormalities in the sizes of the somas, dendritic fields and axons of midget and parasol cells (Weber et al 1998; Quigley 1993). Within the retina the P-pathway cells with medium sized somas project to the parvocellular layers of the LGN. These neurons have small receptive fields and have slow axonal transport velocities; however, they respond best to high spatial and low temporal frequency. In contrast, M-pathway cells have large sized somas, they

project to the magnocellular layers of the LGN, they have large receptive fields and they have fast conducting axons (Dacey and Petersen 1992; Leventhal et al 1981; Rodieck et al 1985). As well, they respond best to high temporal and low spatial frequency.

Axonal flow in retinal ganglion cells of glaucomatous primates is found to be obstructed at the lamina cribosa (Anderson and Hendrickson 1974; Minckler et al 1977, 1978; Quigley and Anderson 1976), and decreased in the magnocellular layers of the LGN (Dandona et al 1991). Glaucomatous atrophy as a result of mechanical damage at the optic nerve head causes a disruption in the flow of intracellular materials in the retinal ganglion cells (Dandona et al 1991; Minckler et al 1977; Quigley and Addicks 1980, Quigley and Anderson 1976). The flow of fast axonal transport ganglion cells appear to be preferentially affected over the slow transport ganglion cells (Dandona et al 1991). As the ganglion cell begin to lose its mode of intracellular signaling, it begins to trim back its distal dendrites to conserve energy and maintain cell homeostasis. Experimentally it was found that the ganglion cells in the glaucomatous primate retina demonstrate a reduction in dendritic arbor, axonal diameter and soma size (Weber et al 1998). Current investigations will determine whether ganglion cells degenerate due to a decrease in interaction with astryocytes (Morgan et al 2000).

iii. Lateral Geniculate Nucleus

The damage seen in the optic nerve appears to translate into the LGN; however, reports examining the LGN of glaucomatous primates have revealed some contrasting findings. Several studies found that both the M- and P- pathways were affected by elevated IOP. This is shown histologically in adult glaucomatous primates with a decrease in the numbers of magnocellular and parvocellular LGN relay neurons (Yucel et al 2000) and decreased staining density of CO histochemistry and synaptophysin (SYN) immunohistochemistry (Crawford et al 2000; Vickers et al 1997). The results of these studies differ from the findings of Chaturvedi et al (1993) and

with the findings from Weber et al (2000) where elevated IOP caused cellular loss to be greater in the magnocellular rather than in the parvocellular regions of the LGN; however, it is suggested that perhaps cell size rather than cell class may be the main factor in glaucomatous changes. Therefore even the "larger" parvocellular cells are affected by this deprivation.

iv. Visual Cortex

Two recent studies have demonstrated contrasting results on the levels of cytochrome oxidase in the primate visual cortex at 1year post-elevated IOP. One study found that there was a greater CO reduction in the P-pathway of layer 4Cβ than in the M-pathway of layer 4Cα (Crawford et al 2000). In contrast another report suggested that there was similar decreases in CO density in both layers 4Cβ and 4Cα (Vickers et al 1997). Neither study investigated other neurochemical changes nor did they look at cortical consequences over a shorter period of time.

E. The Pattern of Ocular Dominance Columns in Primate Visual Cortex

In primates, geniculocortical afferents terminate in layer 4C in a pattern of left and right eye columns. Neurons within a column have similar receptive field properties such as orientation and direction selectivity. Each column has intracortical connections which form an organized unit called an ocular dominance column (Hubel and Wiesel 1972). These columns run parallel to each other and they meet perpendiculat to the extrastriate area (area V2) (Hubel and Wiesel 1972).

i. Cytochrome Oxidase Histochemistry

Cytochrome oxidase (CO) has provided investigators with a technique to examine the functional architecture of the visual cortex. Previously investigators utilized autoradiography, electrophysiology, and or Nissl staining to demonstrate the cytoarchitecture of the visual cortex.

The development of the cytochrome oxidase staining method revealed a major organizational feature of primate striate cortex, the CO blobs (Horton and Hubel 1981; Humphrey and Hendrickson 1983; Wong-Riley 1979).

CO stained tissue is stable across a wide range of pH, temperature and fixation procedures (Seligman et al 1968; Wikstrom et al 1981; Wong-Riley 1979,). It is an integral membrane protein, located on the inner mitochondrial membrane; therefore, it is much more stable than other cytoplasmic proteins (Wong-Riley 1994) and CO labels metabolically active dendritic and axonal terminals. An adequate accumulation of visible reaction product is made by a continual reoxidation of cytochrome c by CO (Wong-Riley 1979). Therefore the intensity of the product demonstrates the cytochrome oxidase activity in the tissue (Hevner and Wong-Riley 1990). As well, it can be used in conjunction with techniques such as autoradiography (Livingstone and Hubel 1982, 1983; Carroll and Wong-Riley 1985, 1987), anterograde or retrograde axonal tracing (Mjaatveldt and Wong-Riley 1988), or 2-deoxyglucose autoradiography (Tootell et al 1985; 1988).

CO has been found to be an advantageous marker of neuron activity (Wong-Riley 1989). It accounts for over 90% of oxygen consumption in living organisms (Wikstrom et al 1981). It plays a critical role in energy metabolism and because the brain depends on aerobic metabolism for its energy supply, it is the ideal candidate to identify functional levels of activity in the cortex (Wong-Riley et al 1978; Wong-Riley 1979). There is evidence that CO activity and functional activity are correlated under normal conditions and there are adaptive adjustment of cellular levels of CO after altered neuronal activity (Wong-Riley 1989).

Layers 2/3

Electrophysiology, autoradiography, and Nissl staining have led to our understanding of ocular dominance columns; however, these procedures have been unsuccessful in revealing the

organizational pattern in layers 2/3 of the visual cortex that can be seen with CO histochemistry. When normal primary visual cortex is histochemically reacted for CO, a pattern of CO-rich zones termed puffs and non-CO-rich zones termed interpuffs is visible (Carroll and Wong-Riley 1984).

CO puffs are oval in shape and have been reported to range in diameter between 150 microns to 377 microns (Horton 1984; Wong-Riley and Carroll 1984). They are aligned in rows and are spaced approximately 550 microns apart along the long axis of the ovals (Horton and Hubel 1981; Humphrey and Hendrickson 1983). Puffs extend throughout the supragranular layers 1-3 (Hendrickson et al 1981; Horton and Hubel 1981; Horton 1984; Trusk et al 1990; Wong Riley and Carroll 1984) and are found to align with the centres of ocular dominance columns (Horton 1984, Horton and Hedley-Whyte 1984; Wong-Riley and Carroll 1984).

CO puffs receive input from all three LGN pathways, direct input from the konicocellular (K) pathway (Diamond et al 1985; Ding and Casagrande 1997; Fitzpatrick et al 1983; Hendry and Yoshioka 1994; Lachica and Casagrande 1992; Livingstone and Hubel 1982; Weber et al 1983;), and indirect input from both the M and P pathways (Lachica and Casagrande et al 1992; Livingstone and Hubel 1984; Yoshioka et a l994).

Layer 4

In the cortex, thalamic layers are found to have high CO activity (Carroll and Wong-Riley 1984). There is a wide range in periodicity of ocular dominance columns in adult monkeys; however, periodicities of contralateral and ipsilateral cortices of each individual animal have been found to be virtually identical (Horton and Hocking 1996). CO staining has demonstrated the various subdivisions in layer 4, highlighting layer 4A and layer 4C as significantly darker than layer 4B.

Tangential sections of CO staining in layer 4A reveal a 'honeycomb-like' pattern (Carroll and Wong-Riley 1984; Hevner and Wong-Riley 1990; Horton 1984;). Layer 4B lacks direct

geniculocortical input therefore CO staining is much lighter in this layer (Livingstone and Hubel 1982). Layer 4C, the geniculocortical input layer, is rich in both CO activity and enzyme amount (Hevner and Wong-Riley 1990). Layer 4C can be divided into 4Cα and 4Cβ with higher CO activity in layer 4Cα than 4Cβ (Liu and Wong-Riley 1990; Wong-Riley and Carroll 1984). The base of 4Cβ sends inputs to layer 4A whereas the upper portion of 4Cβ sends inputs to layer 3B (Fitzpatrick et al 1985). The differential staining within layer 4Cβ has been attributed to the inputs from different layers. 4Cβ dark receives innervation from layer 5 and 6 of the LGN and upper 4Cβ receives innervation from layers 3 and 4 of the LGN (Liu and Wong-Riley 1990).

ii. Effects of monocular deprivation

Monocular lid suturing, TTX injection, enucleation:

Because the primate model of glaucoma involves inducing unilateral elevated IOP, a form of monocular deprivation, it is necessary to understand previously reported monocular deprivation paradigms. The most common ones are lid suturing, TTX injection and enucleation. The organization of the visual cortex with the segregation of left and right eye ocular dominance columns allows direct comparisons between deprived and non-deprived cortical areas within an individual animal. In monocularly deprived primates, CO staining indicates the changes in metabolic activity in the deprived and non-deprived eye. Visual deprivation by monocular enucleation, lid suture and retinal impulse blockade has been shown to lead to a downregulation of CO in the affected ODC of adult monkeys (Hendrickson and Tigges 1985; Hendry and Jones 1986; Horton and Hubel 1981; Horton 1984; Trusk et al 1990; Wong-Riley and Carroll 1984; Wong-Riley et al 1989).

Monocular lid suturing is one of the mildest forms of visual deprivation. After lid suturing of the adult animal, retinal ganglion cells retain their spontaneous activity and the LGN still responds to diffuse light through the lid for at least 6 months (Horton 1984). No changes in

CO pattern are detected in the LGN; however faint CO bands can be seen in layer 4 11 weeks after monocular lid suturing (Horton 1984; Trusk et al 1990). The bands are much more distinct in juveniles than in adults; however, the effects become more prominent with longer deprivation periods of 1-3 years (Trusk et al 1990). Transneuronal labeling studies demonstrated that there is no sprouting or contraction of geniculocortical afferents in the adult animal (Horton 1984; LeVay et al 1980). In layers 2/3, rows of lightly stained CO puffs correspond with light CO columns in layer 4 (Horton 1984; Trusk et al 1990) and puff volumes are significantly reduced at 11 weeks post lid suture (Trusk et al 1990). In layers 5 and 6, patchy staining is also evident, indicating a deprivation effect on all cells throughout the entire extent of the cortex (Horton 1984; Trusk et al 1990).

Deprivation by monocular enucleation demonstrates a dramatic effect on CO histochemistry. When one eye is removed, transneuronal degeneration in the mature postsynaptic LGN neurons is observed (Matthews et al 1960) and increased cellular density is seen in layer 4C of Nissl-stained sections (Hazeltine et al 1979; Hendrickson and Tigges 1985). As well, the metabolic activity in the deprived-eye columns is severely reduced as revealed by pale CO staining in deprived eye columns (Horton and Hedley Whyte 1984; Hess and Edwards 1987; Horton and Hubel 1981; Horton 1984; Trusk et al 1990). In layer 4C, there are alternating rows of pale CO (enucleated eye) and dark CO (normal eye) stained ocular dominance columns and the darkly stained columns are significantly wider than the lightly stained columns (Trusk et al 1990). In layer 2/3, alternating rows of puffs becomes paler and smaller in the deprived eye columns as compared to the normal eye rows of CO puffs (Horton 1984).

Tetrodotoxin (TTX) is a specific blocker of voltage dependent sodium channels. Intravitreal injections of TTX does not cause cell death nor does it interfere with axoplasmic transport (Wong-Riley and Riley 1983). During monocular deprivation by TTX injection, the

eyelids remain open so that light can still enter both the injected and noninjected eye. There is no permanent damage to the system as the process is reversible and enzymatic activity can return to normal (Wong-Riley and Riley 1983; Wong-Riley et al 1989). In primate, pale ocular dominance bands are seen in layer 4C, 14 hours after TTX injection (Wong-Riley 1994). Longer deprivation periods results in the light and dark CO bands in layer 4C and the alternating rows of pale shrunken puffs in layers 2/3 (Hevner and Wong-Riley 1990). Different from monocular enucleation, deprivation by TTX injection results in equal widths of light and dark ODCs in layer 4C (Trusk et al 1990).

The effects of monocular deprivation by TTX or enucleation is detectable within 4 days post-deprivation; however, the effects of lid suture is not detectable until 4-6 weeks post-deprivation. Cell counting reveals that there is no significant cell death in layer 4C after TTX injection (Hendry and Jones 1988); however, there is cell shrinkage as revealed by Nissl staining (Haseltine et al 1979). In adults, monocular TTX and enucleation will result in a pattern of large blobs overlying the darkly reactive ocular dominance bands. In monocular lid suture animals, this pattern is less visible in adults (Trusk et al 1990).

F. Neurochemicals associated with cortical plasticity

Cortical plasticity can be defined as the ability to make adaptive changes in response to peripheral lesions (Bloom 1985). It has been hypothesized that adaptive changes may occur in neurons or in their synapses or receptors. This study is focused on whether peripheral deafferentation by elevated IOP will result in changes in a variety of neurochemicals that have been associated with cortical plasticity.

i. Growth associated protein – 43 :

GAP-43 is a 226 amino acid protein (Basi et al 1987; Cimler et al 1987; Karns et al 1987), which is found on the axon shaft and the membrane of cell soma (Goslin et al 1988; Van

Hoff et al 1989; Zuber et al 1989). Immunohistochemical studies have shown that in the adult brain, GAP-43 is found in regions rich in synapses (Benowitz et al 1988; Benowitz et al 1989; De La Monte et al 1989; DiFiglia et al 1990) and is neuron specific in expression (Basi et al 1987; Biffo et la 1990; Karns et al 1987). Regional variation in GAP-43 expression exists within the CNS (Neve et al 1987). In the primate visual system, GAP-43 is lowest in the striate cortex and highest in regions associated with memory storage (Nelson et al 1987). Immunohistochemical distribution of GAP-43 in adult cat and human visual cortex is laminar.

GAP-43 is found to be associated with axon elongation (Jacobson et al 1986; Karns et al 1987; Skene and Willard 1981a, 1981b; Zuber et al 1989), and is believed to be critical for axonal growth (Meiri et al 1986; Skene et al 1986). Because GAP-43 expression has been found in the hippocampus of rodents and in the association cortex of humans, it is possible that it is involved in the remodeling that accompanies learning and memory (Benowitz et al 1988, 1989) suggesting that GAP-43 is increased in nerves that are growing axons or otherwise remodeling connections. Its protein expression is found to increase after neuronal injury (Benowitz and Lewis 1983; Doster et al 1991; Hoffman 1989, Ng et al 1988; Schreyer and Skene 1991). It has been shown that neurons which express high levels of GAP-43 in the adult are capable of synaptic remodelling olfactory nerve and its target (de la Monte et al 1989; Jacobson 1978)

It is not unreasonable that a molecular mechanism is needed to remodel synapses in the mature nervous system. Therefore, restricted localization of GAP-43 in the adult CNS would be compatible with the notion that GAP-43 expressing neurons are those actively engaged in nerve terminal remodeling. In binocular retinal lesion experiments in the adult cat, deprivation periods of 8 months resulted in an increase in GAP-43 immunoreactivity in the area of the LGN which corresponded to the lesioned area of the retina (Baekelandt et al 1994, 1996). Interestingly, an

elevation of GAP-43 immunoreactivity was not observed in the lesioned area of the visual cortex (Baekelandt et al 1994, 1996)

ii. Synaptophysin:

Synaptophysin (SYN), a presynaptic vesicle membrane glycoprotein, is located on the cytoplasmic surface of the vesicle (Buckley et al 1987; Sudhof et al 1987). During development, the expression of SYN increases in parallel with the formation of synapses (Kanus et al 1986) and SYN immunoreactivity matches synaptic profile distribution (Voigt et al 1993). Biochemical quantification of SYN (Brock et al 1987; Walaas et al 1988) following lesions in the rat brain has shown that the levels of these synapse markers can be used to quantify presynaptic terminals in the CNS.

SYN and GAP-43 levels are increase in the rat dentate gyrus after perforant path transection. (Masliah et al 1991). As well, further investigations showed that some terminals had GAP-43 present, but no anti-SYN labeling suggesting that SYN is expressed once the presynaptic terminals has become stable and contain newly synthesized synaptic vesicles.

iii. γ-aminobutyric-acid

GABA is a major inhibitory neurotransmitter of the mammalian cerebral cortex (Krnjevic 1984) and most of the inhibitory actions are mediated through the GABAa receptor. The GABA synthesizing enzyme is glutamic acid decarboxylase (GAD). It was found in adult primate cortex that the regulation of GABA neurotransmitter and its receptor is dependent on visual activity (Hendry and Jones 1986, 1988).

<u>GABA and GABAa Receptor</u>

GABAergic neurons as well as the synthetic enzyme GAD, are found throughout the 6 layers of the cortex in area V1; however, their distribution is not uniform. GABAergic neurons and GAD are most abundant in layers 2/3, 4A, and 4C (Fitzpatrick et al 1987; Hendry and Jones

1986). GABA, GAD and the GABAa receptor (α, β, γ subunits) are found in high density in layers 2/3, 4A and 4C, moderately dense in layers 1 and 6 and sparsely dense in layers 4B and 5 (Fitzpatrick et al 1987; Hendrickson et al 1981; Hendry et al 1990; Huntsman et al 1991; Rakic et al 1988; Shaw and Cynader 1986;). Within layer 4C, there is a sublaminar distribution of GABA and its receptors. Both GABAergic neurons and the GABAa (β subunit) receptor are more densely distributed in layer 4Cβ than in layer 4Cα (Fitzpatrick et al 1987; Hendry et al 1990; Hendrickson et al 1981).

The pattern of GABA staining in adult area V1 can change dramatically after monocular deprivation. Monocular deprivation for at least 4 days by intravitreal injections of tetrodotoxin (TTX), or enucleation results in a pattern of alternating light and dark immunostained GABA bands which coalign with the light and dark CO bands (Hendry and Jones 1986). Monocular lid suturing on the other hand does not cause changes in GABA immunoreactivity until more than 2 months later (Hendry and Jones 1986, 1988), indicating that silencing or removing retinal activity provides a much more dramatic deprivation effect. Along with GABA and GAD immunoreactivity reduction, the GABAa receptor is also found to be downregulated in deprived eye columns of layer 4Cβ as measured by radioligand labeling and immunohistochemistry studies (Hendry et al 1990).

iv. Calcium-calmodulin dependent kinase II α:

CAMKIIα is a major postsynaptic density protein (Kennedy et al 1983; Kelly et al 1984) and is associated mainly with excitatory synapses (Benson 1991a). Its distribution is most dense in layers 2/3, 4B and 5 and less dense in layers 4A, 4C and 6 (Hendry and Kennedy 1986).

CAMKIIα has been found to be involved with phosphorylating structural proteins (MAP2) (Kelly et al 1984, Miller and Kennedy 1985, Schulman 1984, Vulliet et al 1984), with synaptic vesicle movement (McGuinness et al 1989) and with transmitter related and other

neuronal enzymes (Bennet et al 1983; Bulleit et al 1988; Schulman 1984; Yamaguchi and Fugisawa 1983). It is a critical downstream step after influx of Ca^{2+} through the NMDA channels (Llinas et al 1985; McGuinness et al 1989). Its involvement in hippocampal and visual cortical LTP is demonstrated in a mouse with a CAMKIIα knockout gene where no significant hippocampal nor visual cortical LTP occurred (Kirkwood et al 1997; Silva et al 1992).

Monocular deprivation results in alternating rows of light and dark CAMKIIα immunoreactivity and mRNA in layer 4C (Hendry and Kennedy 1986). Differential mRNA levels between the deprived and non-deprived columns are less distinguishable 15 days post-deprivation; however CAMKIIα proteins demonstrate a more prolonged increase (Hendry and Kennedy 1986). Interestingly, the light immunostained CAMKIIα bands coalign to the dark CO bands a pattern which differs from the localization seen with GABA immunohistochemistry (Hendry and Kennedy 1986). Its role in ocular dominance formation is seen in CAMKIIα knockout animals where there is a decrease in ocular dominance shifts after monocular deprivation (Silva et al 1992).

G. Effects of Elevated IOP on Neurochemical Markers in the Adult Visual Cortex – An Hypothesis:

Studies on monocular deprivation have demonstrated both metabolic and neurochemical changes at the level of the LGN and the visual cortex in adult primates (Hendry 1991; Tigges et al 1994; Tighlet et al 1998). Monocular deprivation paradigms have typically included lid suturing, monocular TTX injection or enucleation. Procedures which results in unilateral elevated IOP leaves the primate eye remain intact. It causes apoptosis of retinal ganglion cells, cupping of the optic disc and reduction of visual field (Harwerth et al 1999; Kerrigan et al 1997; Varma et al 1992). The primate eyes remain open, and can still perceive visual forms, which makes elevated IOP unlike monocular lid suturing. At the level of the eye, monocular

deprivation by elevated IOP partially resembles monocular TTX injection. Both result in silencing impulse activity and disrupting axoplasmic transport, the former is caused by retinal ganglion cell death and the latter is caused by tetrodotoxin. Although, unlike monocular TTX deprivation, the 'interruption' in ganglion cell activity is not reversible. In this one respect, one might suggest that monocular deprivation by elevated IOP resembles monocular enucleation; however, that is not enough to draw parallels to this third paradigm. Removal of the entire eye, which involves severing the optic nerve is much more dramatic than elevated IOP. Therefore amongst these three paradigms, deprivation by elevated IOP is most similar to monocular TTX injection; however, its effects are likely to be more severe because it involves cell death and interruption of axoplasmic transport, both of which do not occur with TTX injections. Given previous studies on the effects of monocular TTX injections in the visual cortex, we hope to be able to correlate CO histochemistry with immunohistochemical staining from four other neurochemicals so that we can analyze the spatial distribution of neurochemicals in adult visual cortex in response to elevated IOP.

While this study was in progress, other investigators reported changes in LGN cell numbers (Yucel et al 1999), changes in cortical CO levels (Crawford et al 2000) and changes in LGN soma size (Weber et al 2000) after elevated IOP. However, evidence for spatial redistribution of neurochemicals after elevated IOP has not been obtained. The present study examines the levels of four neurochemical markers in the adult primate visual cortex after monocularly inducing elevated IOP. The density levels of these neurochemical markers in deprived animals will be compared to density levels in normal (non-deprived) animals. And because the animals will be treated to monocular elevated IOP, the density levels corresponding to the deprived eye cortical columns will be compared to density levels corresponding to the non-deprived eye column of each animal.

Four neurochemical markers have been chosen in our study, GAP-43, SYN, CAMKIIα and GABAa receptor. These are neurochemicals which have been used in adult visual cortex and have been found to be differentially expressed post monocular deprivation. We hypothesize that neurochemical changes will be detected in the primary visual cortex of primates with elevated IOP. We expect to find a higher density of GAP-43, SYN and CAMKIIα in the glaucomatous animals versus normal animals because two of these proteins are reported to be associated with growth of axons and synapses during development (Kanus et al 1986; Meiri et al 1986; Skene and Willard 1981a) and the third is reported to be involved with LTP and with ocular dominance plasticity during development (Gordon et al 1996; Malenka et al 1989). Therefore in response to the deprivation the increased levels of GAP-43 and SYN would suggest potential changes in axonal growth or potential changes in synaptogenesis while the increase in CAMKIIα would suggest that plastic changes are being mediated in the cortex. Meanwhile, as GAP-43, SYN and CAMKIIα protein levels increase, we hypothesize that the GABAa receptor protein levels, would decrease in response to elevated IOP. Hendry et al 1991 has demonstrated in adult primates that GABAa receptor protein levels are activity dependent and a reduction in this inhibitory neurotransmitter receptor would suggest that excitatory mechanisms such as axonal growth and synaptogenesis could be occuring in response to elevated IOP.

Although all four neurochemicals have been used in either the LGN or the cortex during adult monocular deprivation studies (Baekleandt et al 1994, 1996; Hendry and Kennedy 1986; Hendry and Jones 1986; 1988; Tighlet et al 1998, Vickers et al 1997), this study is unique in that these neurochemicals have not been examined in conjunction with elevated IOP and their spatial distribution has not been examined over three different deprivation periods.

2. Materials and Methods

A. Animal Preparation

i. Surgery

A total of 10 monkeys was used for this study (Table 1). All animals were treated at the University of Wisconsin Department of Ophthalmology. Seven monkeys (5 rhesus and 4 cynomologous) were treated to unilateral elevated intraocular pressures (IOP) for periods of 2, 4 and 7 months by laser ablation to their trabecular meshwork. Two other monkeys, which did not have their trabecular meshwork laser ablated, served as normal controls and a tenth monkey did have its trabecular meshwork laser ablated, but its IOP levels were relatively normal and thus served as a sham operated control (Table 1). A standard clinical argon laser and slit lamp delivery system was used to produce a series of focal lesions to the trabecular meshwork in one eye (75 to 250 spots, 50 μm spot diameter, 1-1.5 W, 0.5 seconds duration). IOP was monitored every few days for 2 to 3 weeks after treatment, and if not consistently above 30-40 mm Hg, additional laser treatments were performed until a stable ocular hypertension was achieved. IOP was checked weekly thereafter to assure stability and additional laser treatment or IOP-lowering therapy was applied as needed to control the IOP levels. The opposite eye served as a normal control. IOP levels in this study ranged from 30-66 mmHg. After the designated periods of IOP elevation, animals were euthanized and perfused intracardially with 750ml posphate buffer saline (PBS), followed by 1 litre of 4% paraformaldehyde and again with 200-300 ml PBS. The brains were excised and shipped in 4% paraformaldehyde at 4° Celsius to UBC (Figure 4).

B. Tissue Preparation

i. Blocking, Flattening and Sectioning

Before flattening, the pia was removed from the surface of each brain. The striate cortex, was flattened and cryoprotected in 20% sucrose solution. The method of flattening as described

Figure 4: Materials and methods schematic
(#) number of animals – indicates the number of animals used at each step

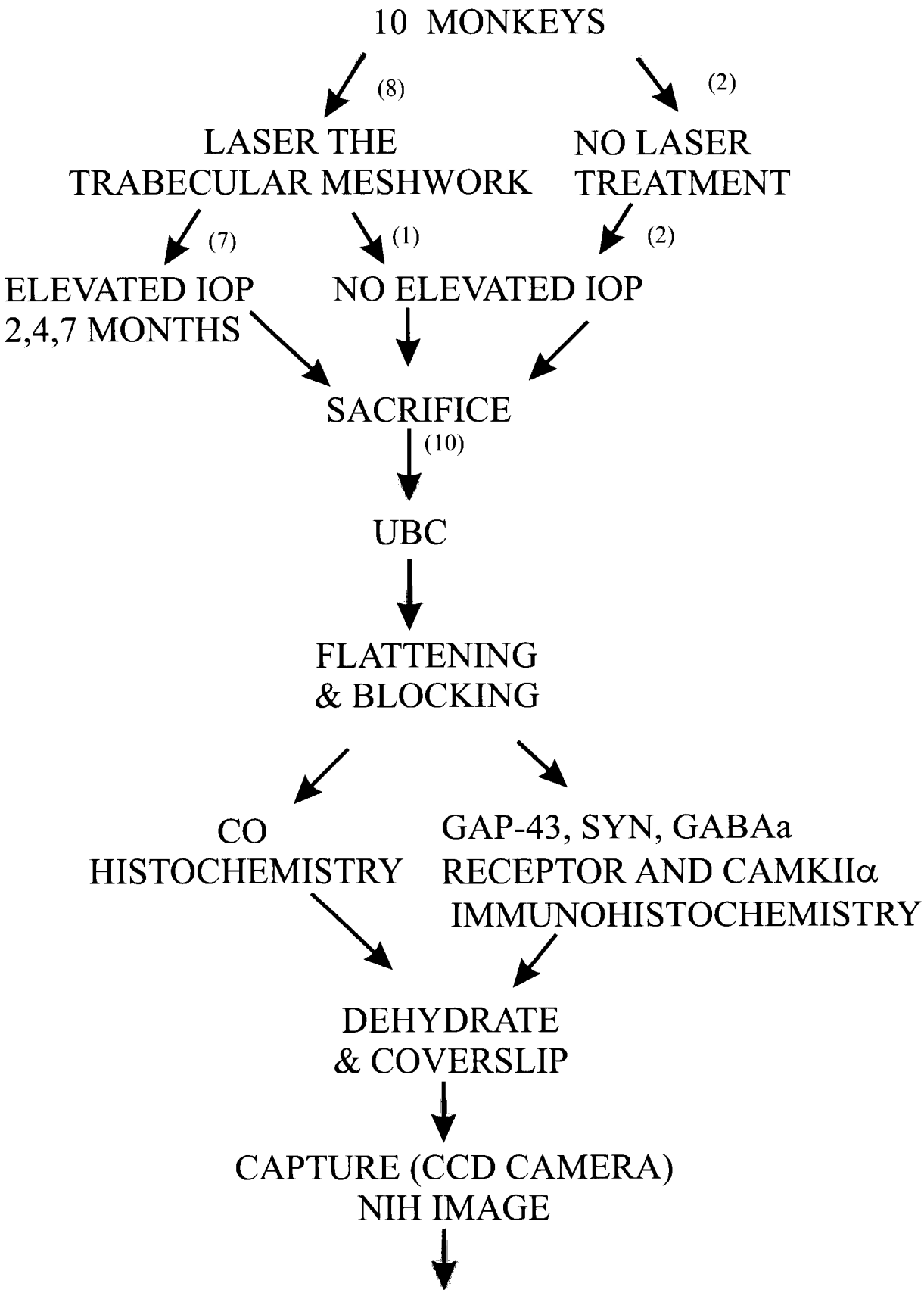

(#) number of animals

by Horton and Hocking (1996) demonstrates major geographical features in the visual cortex (Figure 3). The cortical areas at the operculum, the calcarine sulcus and calcarine fissures can be flattened so that ocular dominance columns in these areas can be analyzed histochemically. The operculum, located at the most posterior aspect of the occipital lobe, is a fairly flat and smooth piece of cortex that is separated from the calcarine sulcus and calcarine fissure into a single cortical region which we have labeled block 1 and block 2 (Figure 3). Block 1 represents the most superficial region of the operculum and block 2 represents the internal folds of the calcarine sulcus. The remaining area of the visual cortex located within the calcarine sulcus and along the calcarine fissure (LeVay et al 1985; Kennedy et al 1975; LeVay et al 1980; Van Essen et al 1984) can be divided further into blocks 3 and 4 (Figure 3). A 'hinge' area separates the operculum surface from the calcarine block which consists of the 'roof' (block 2) of the calacrine sulcus, the ventral bank (block 3) and the dorsal bank (block 4) of the calcarine fissure (Figure 3). A #10 scalpel blade was used to make an incision to extend the calcarine sulcus, parallel to the opercular surface (Figure 3). The lunate sulcus and the inferior occipital sulcus, two of the sulci which borders the posterior occipital lobe, were probed gently by a metal spatula. At the most lateral tip of block 1, an incision was made to extend the lunate sulcus to the inferior occipital sulcus so that the opercular part of the visual cortex could be removed. The operculum (blocks 1 and 2) was separated from the rest of the cortex by cutting down the calcarine sulcus along the white matter. The resulting block is a relatively flat triangular piece of cortex (Figure 3). Further, the rest of VI is dissected out by spreading apart the calcarine fissure and dissecting out blocks 3 and 4 parallel to the pia surface of the fissure (Figure 3).

C. Histochemistry

Histology on all 10 monkey brains was not undertaken at the same time; therefore, upon arrival at UBC, each block of cortex was cryoprotected and kept frozen at -80 deg Celsius before

histology was performed. All tissue blocks were cryoprotected in 20% sucrose made in phosphate buffer (PB). The visual cortices were gently flattened tangentially between 2 glass slides before being frozen on dry ice. Tissue was stored at -80° C until ready for use. All sections were cut at 50 μm on the freezing microtome. Every third section was reacted for cytochrome oxidase (CO) or immunohistochemically for growth associated protein (GAP-43), SYN (SYN), GABAa receptor (β2/3 subunit) or calcium-dependent protein kinase II α subunit (CAMKIIα).

i. Cytochrome oxidase

The cytochrome oxidase reaction was adapted from other authors (Wong-Riley 1989; Boyd and Matsubara 1996). First, 20 mg of diaminobenzidine (DAB) (Sigma-Aldrich Co) was dissolved in 50 mL of distilled water. Once dissolved, 50 mL (0.1M) PB, 2 g of sucrose, 30 mg cytochrome C (Sigma-Aldrich Co) and 20 mg of catalase (Sigma-Aldrich Co) derived from bovine heart were added to the DAB solution. Then, 5 ml of (1%) nickel ammonium sulfate was added dropwise followed by approximately 1 ml of (1%) cobalt chloride until the solution appeared slightly opaque. Sections were placed into 12 well plates filled with 1.5 ml of the cytochrome oxidase solution.and incubated at 40° C for 3-6 hrs. Upon completion of the reaction, the sections were washed 3x for 5 min each in PB.

D. Immunohistochemistry

The spatial distributions of four neurochemical markers (GAP-43, SYN, GABAa receptor, CAMKIIα) in relation to normal and deprived ocular dominance bands was studied. Sections from the left hemisphere were reacted histochemically for CO, and immunohistochemically for GAP-43 and for the GABAa receptor (β chain). Sections from the right hemisphere were reacted histochemically for CO and immunohistochemically SYN and CAMKIIα.

i. GAP-43, SYN, CAMKIIα, GABAa Receptor

Monoclonal antibodies against GAP-43 (Sigma-Aldrich Co), SYN (Sigma-Aldrich Co), CAMKIIα (Boehringer-Mannheim) and the GABAa (Boehringer-Mannheim) receptor were used in this study. For GAP-43, SYN, and the GABAa receptor, immunostained sections of primary visual cortex and frontal cortex were incubated in 5-10% normal horse serum (NHS) for 1 hour to block for non-specific binding. Sections were then washed 3x for 5 min each in PB. GAP-43 and SYN antibodies were used at a 1:2000 dilution in 3% NHS in 0.1% TX 100 made in PB. Antibody against GABAa receptor was used at a 1:200 dilution in 3% NHS in 0.1% TX100. CAMKIIα immunostained sections (Boehringer Mannheim) were preincubated in 0.2% TX100 for 15 min before incubating in a 1:1000 dilution in 3% NHS in 0.1% TX100. All immunostained sections were agitated and incubated at 4° C in primary antibody for 36-48 hrs. Sections were washed 3x for 5 min each in 0.1% TX100 before being incubated for 2 hrs at room temperature in 0.1% secondary antibody, biotinylated anti-mouse made in horse, in 3% NHS in 0.3% TX100 made in PB. Prior to incubation with the avidin biotin complex for 1 hr, sections were washed 3x for 5 min each in PB. Antibodies were visualized using the glucose oxidase-diaminobenzidine reaction where 10mg of diaminobenzidine, 40 mg dextrose and 8 mg of ammonium chloride were dissolved in 20mL of PB. Sections were pre-incubated in this diaminobenzidine reaction for ten minutes before the addition of glucose oxidase (6 mg glucose oxidase in 50 mL distilled water). Glucose oxidase was added to the DAB solution at a 1:10 ratio and the reaction proceeded in the dark for 30-60 mins before being halted by rinsing 3x in PB for 5 mins. Sections were mounted on gelatin coated slides, air dried and dehydrated through an ascending concentration of alcohols before being cleared in xylene and coverslipped in Permount (Sigma). Control sections for each marker utilized the same protocol except the primary antibody was omitted.

E. Data Collection and Analysis

i. Image Capturing

Video images were captured on an Aristo brand light box with a COHU CCD (4915) camera attached to a Nikon micro NIKKOR 55mm lens. The camera was connected to a Macintosh IIfx-based analysis system with a Data Translation DT-2255 quick capture board. The setting on the light box and F-stop of the lens remained constant throughout at 100 and f16 respectively. NIH Image 1.62 was used to obtain density profiles and to measure periodicity of ocular dominance columns. Raw OD values were converted to a linear index standardized by using neutral density filters.

ii. Inter-animal Analysis

Our first analysis was to determine whether there were any changes in neurochemical levels between glaucomatous animals and normal (non-deprived) animals at the three deprivation periods of this study. A comparison between normal tissue and experimental tissue was required, but because normal tissue was not available to us until part way through the study we could not react normal animal tissue simultaneously with glaucomatous animal tissue. We developed a method of normalizing our data because immunohistochemical staining can vary from one animal to the next. For each of the 10 monkey brains we had access to their frontal cortex (other parts of the cortex were shipped to another lab in Toronto). We assumed that neurochemical densities did not fluctuate significantly in the frontal cortex in response to elevated IOP; therefore, by comparing the neurochemical densities in the visual cortex to the densities in the frontal cortex of each animal, a ratio of visual to frontal cortex was derived for normal and glaucomatous animals.

The frontal cortex was coronally blocked at stereotaxic coordinates between A25.0 – A35.0. Sections of frontal cortex were processed with sections of visual cortex to ensure

constant staining conditions. For experimental animal tissue, the visual cortex was cut tangentially and, for normal animal tissue, the visual cortex was cut coronally.

Transects were placed perpendicularly, from pia surface to white matter of frontal cortex, to measure optical density (OD) and then an average was taken of these values for all four neurochemical markers (Figure 5). In visual cortex, optical density was measured in layer 4C for all four neurochemical markers and the average for each neurochemical marker was normalized to a mean frontal optical density value. In normal animals, the transects were placed parallel to the pia surface and at least 30 such measurements were collected per animal for each neurochemical marker. In glaucomatous animals, optical density measurements were made in dark and light immunostained bands of layer 4C and at least 30 such measurements were collected per animal for each neurochemical marker. Normalized visual cortex protein densities from normal animals were then compared to those from experimental animals in an attempt to determine if the levels of GAP-43, SYN, GABAa receptor and CAMKIIα were increased or decreased after deprivation.

iii. Intra-animal Analysis

Our second type of analysis was to determine if elevated IOP causes specific changes in neurochemical levels between the deprived and non-deprived eye columns. To determine whether the dark immunostained bands represented the deprived or non-deprived eye columns, immunostained sections were co-aligned to adjacent CO-stained sections using radial blood vessels to align serial sections. Transects were centred over dark immunostained bands and in adjacent light immunostained bands, taking care to avoid border regions (Figure 6). Because we were comparing the density between adjacent deprived and non-deprived eye bands, the difference between the two is expressed by subtracting the deprived eye OD value from the non-deprived eye OD value and dividing this difference by the non-deprived eye OD value. For each

Figure 5: Measurements of Optical Density – A. Normal vs Glaucomatous Cortex. Comparing neurochemical densities between normal and glaucomatous animals. The visual and frontal cortices of normal and glaucomatous animals are treated similarly. Frontal and visual cortices of 50 μm are reacted together in the same staining well (Cortical Blocking), immunohistochemisitry is performed and a ratio of visual to frontal cortex is determined (Normalization). If the V/F ratio is smaller in normal animals as compared to glaucomatous animals, then there is an upregulation of neurochemical marker in the glaucomatous visual cortex. If the V/F ratio is in normal animals as compared to glaucomatous animals, there is a downregulation of neurochemical marker in the glaucomatous visual cortex. Lastly, if there is no change in the levels of neurochemical marker between the normal and glaucomatous animals, then there is no change in the levels of neurochemical marker in the glaucomatous visual cortex.

Measurements of Optical Density

A. Normal vs Glaucomatous Cortex

Normal Animal

Cortical Blocking

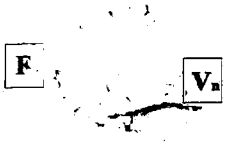

Immuno-histchemistry

Normaization

$$\frac{V_n}{F}$$

Legend

- ☐ Frontal Cortex (**F**)
- ☐ Non-deprived eye Visual Cortex (**Vnd**)
- ☐ Deprived eye Visual Cortex (**Vd**)

Glaucomatous Animal

Cortical Blocking

Immuno-histochemistry

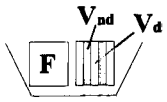

Normalization

$$\frac{V_{nd}}{F}$$

$$\frac{V_d}{F}$$

Ratios of normal (V/F) vs glaucomatous animals (V/F)
Three possible scenarios

$$\frac{V_n}{F} < \frac{V_{nd}}{F} \quad \frac{V_d}{F}$$

Upregulation of neurochemical marker in the glaucomatous visual cortex

---

$$\frac{Vn}{F} > \frac{Vnd}{F} \quad \frac{Vd}{F}$$

Downregulation of neurochemical marker in the glaucomatous visual cortex

---

$$\frac{Vn}{F} = \frac{Vnd}{F} \quad \frac{Vd}{F}$$

No change in the levels of neurochemical marker in the glaucomatous visual cortex

Figure 6: Measurements of Optical Density – B. Deprived vs Non-deprived Eye Columns. Comparing optical density in deprived eye vs non-deprived eye columns. Deprived eye columns were lightly stained under CO histochemistry and GAP and SYN immunohistochemistry. However, deprived eye columns were darkly stained under CAMKIIα immunohistochemistry. Non-deprived eye columns were darkly stained under CO histochemistry and GAP and SYN immunohistochemistry, but lightly stained under CAMKIIα immunohistochemistry. **A.** Differential staining from CO histochemistry and immunohistochemistry in layer 4C. **B.** Transects were placed well within each eye column and optical density was measured. **C.** Optical density from adjacent pairs of dark and lightly stained were compared by subtracting the optical density of lightly stained columns from darkly stained columns and taking it as a ratio over optical density from darkly stained columns.

Measurements of Optical Density

B. Deprived vs Non-deprived Eye Columns

A

Layer 4C, light and darkly stained eye columns

B

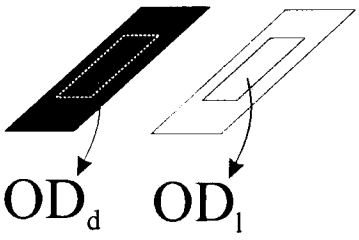

Transects placed within the lightly stained columns and in adjacent darkly stained columns to measure optical density

C

$$\frac{OD_d - OD_l}{OD_d}$$

Difference between dark and lightly stained columns

Figure Legend

OD_d = Optical Density of darkly stained column

OD_l = Optical Density of lightly stained column

animal, a total of more than 30 pairs of transects were collected for each neurochemical and the average for that neurochemical was calculated at each deprivation period

iv. Statistics

Differences in optical density for deprived and non-deprived eye columns as well as differences between optical density for glaucomatous and normal animals were assessed by using repeated measures within factor analysis of variance followed by post hoc comparisons (Fisher). For these statistics, mean differences meeting or exceeding probability value of 0.001 were considered significant.

3. RESULTS

A. Sham operated animal (1720)

Animal 1720 underwent laser scarification, but maintained normal IOP levels of 20 ± 3 mmHg in each eye. The CO staining in layers 2/3 appeared normal and there were no dark and light CO bands in layer 4C (Figures 7A, B) indicating that in this primate model, a sufficiently elevated IOP is needed to cause changes in metabolic activity levels of visual cortex. Immunohistochemistry did not reveal any fluctuation in staining for the four neurchemicals studied here (Figures 8A, B, 9A, B, 10A, B, 11A, B).

B. Experimental animals – Inter-animal Comparisons

i. Two Months post-elevated IOP

Cytochrome oxidase

At two months post-elevated IOP, alternating dark and light CO bands were found in layer 4C of all visual field representations (Figure 7D). In layer 2/3 a regular pattern of CO puffs was observed (Figure 7C).

Figure 7: Cytochrome oxidase (CO) Histochemistry. CO histochemistry in layers 2/3 (**A, C, E, G**) and in layer 4 (**B, D, F, H**). CO was reacted on animals who were sham operated (**A,B**), two months post-elevated IOP (**C,D**); four months post-elevated IOP (**E,F**); and seven months post-elevated IOP (**G,H**). For each time period these two layers were aligned using blood vessels as landmarks (red arrows). The CO blob pattern seen in the sham operated (**A**) and the two months post-elevated IOP animals (**C**) differ from the pattern seen in the four months (**E**) and seven months post-elevated IOP animals (**G**). At four and seven months post elevated IOP rows of pale shrunken CO blobs alternate with rows of more robust CO blobs. In layer 4, CO bands are seen starting from two months post elevated (**D**) to seven months post elevated IOP (**F, H**).

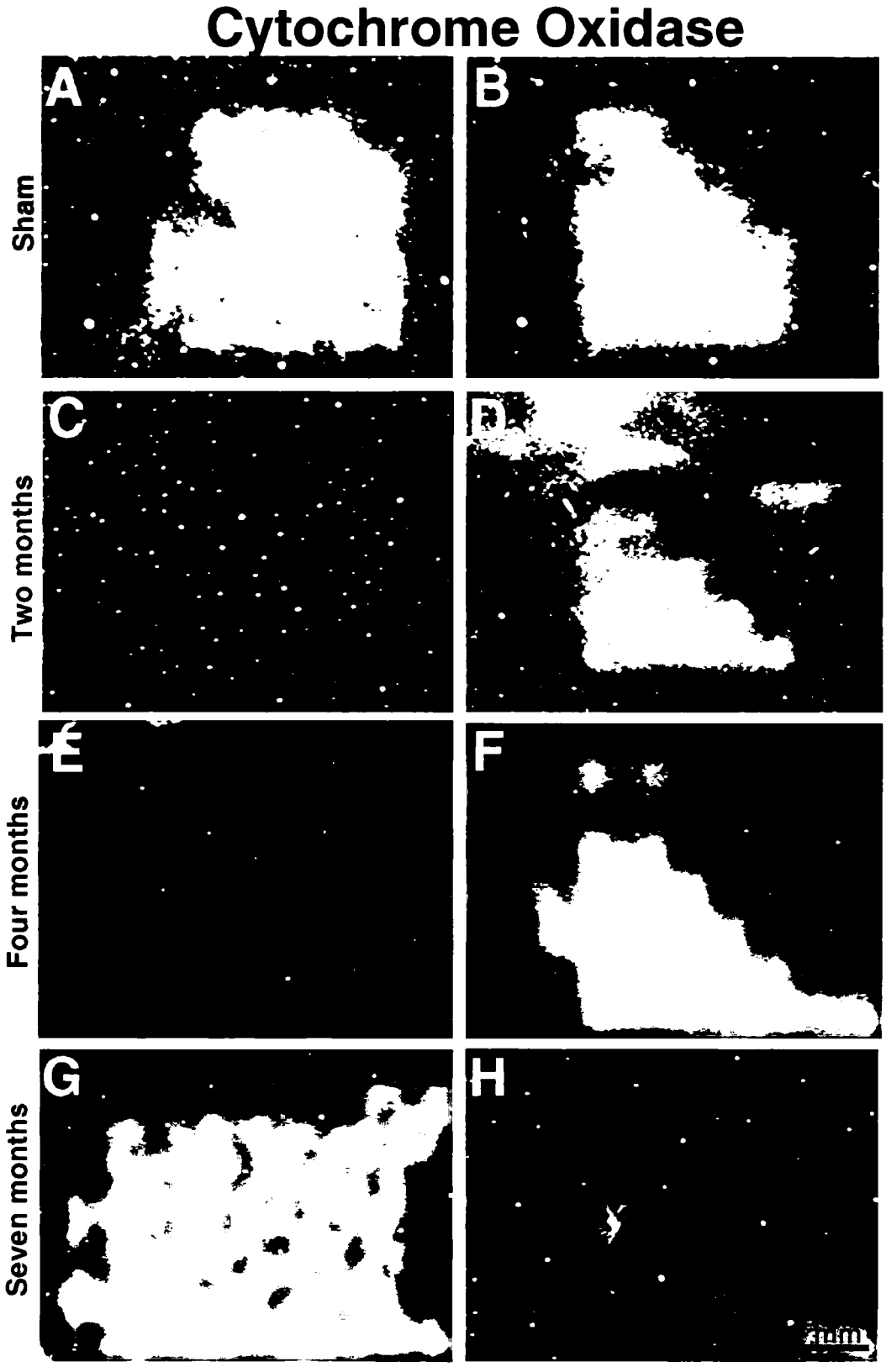
Cytochrome Oxidase
A
B
Sham
C
D
Two months
E
F
Four months
G
H
Seven months

Figure 8: Growth Associated Protein-43 (GAP-43). CO histochemistry in layers 2/3 (**A, C, E, G**) and GAP-43 immunohistochemistry in layer 4 (**B, D, F, H**). GAP-43 was reacted on animals who were sham operated (**A,B**), two months post-elevated IOP (**C,D**); four months post-elevated IOP (**E,F**); and seven months post-elevated IOP (**G,H**). For each time period these two layers were aligned using blood vessels as landmarks (red arrows). GAP-43 bands are absent in the sham-operated animal (**B**); however, it is present in the two (**D**), four (**F**) and seven (**H**) months post-elevated IOP animals.

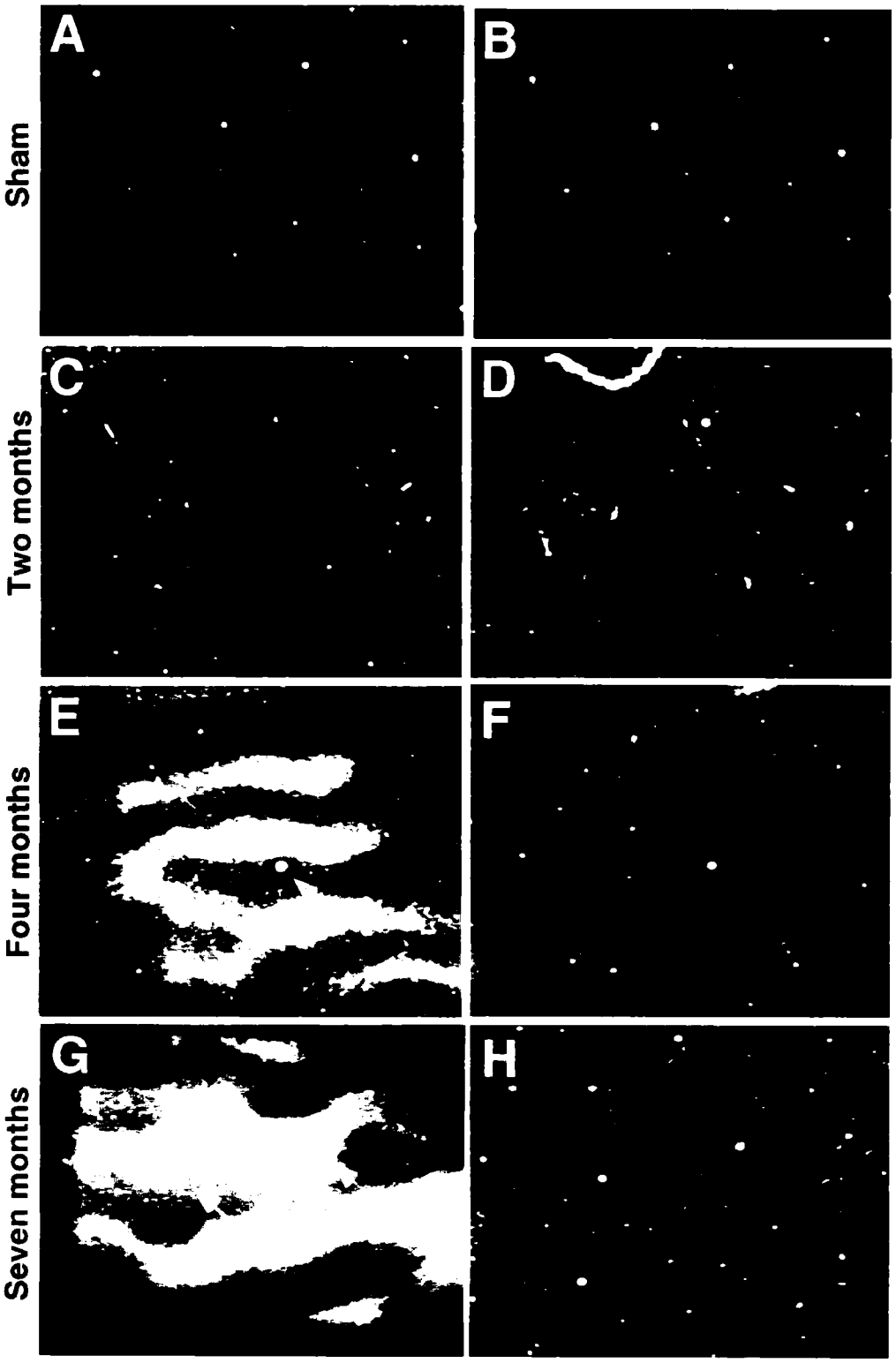
Growth Associated Protein-43
A
B
Sham
C
D
Two months
E
F
Four months
G
H
Seven months

Figure 9: Synaptophysin (SYN) immunohistochemistry. CO histochemistry in layers 2/3 (**A, C, E, G**) and SYN immunohistochemistry in layer 4 (**B, D, F, H**). SYN was reacted on animals who were sham operated (**A,B**), two months post-elevated IOP (**C,D**); four months post-elevated IOP (**E,F**); and seven months post-elevated IOP (**G,H**). For each time period these two layers were aligned using blood vessels as landmarks (red arrows). SYN bands are absent at all time periods except at four months post-elevated IOP (**F**).

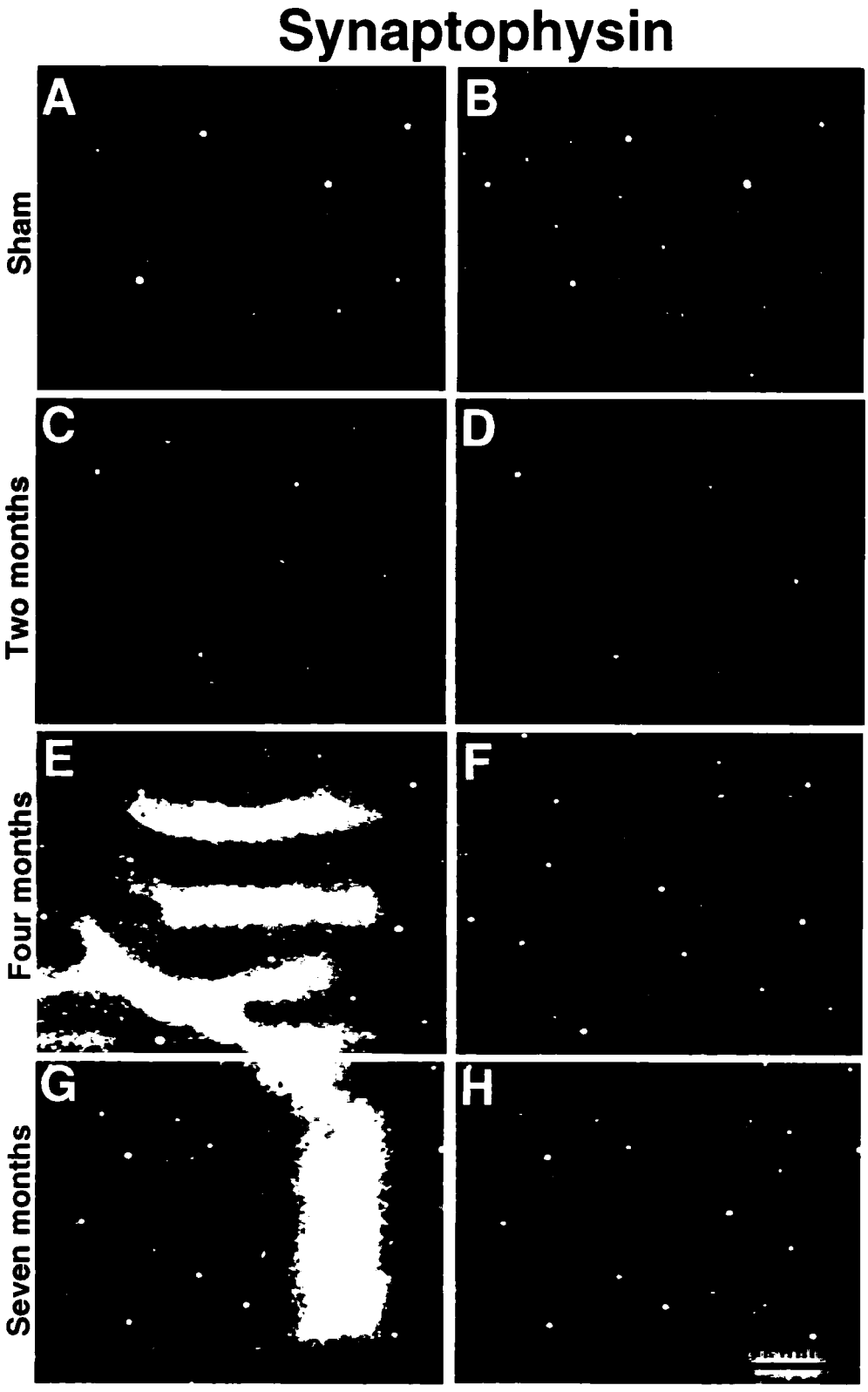
Synaptophysin
A
B
Sham
C
D
Two months
E
F
Four months
G
H
Seven months

Figure 10: GABAa receptor immunohistochemistry. CO histochemistry in layers 2/3 (**A, C, E, G**) and GABAa receptor immunohistochemistry in layer 4 (**B, D, F, H**). GABAa receptor was reacted on animals who were sham operated (**A,B**), two months post-elevated IOP (**C,D**); four months post-elevated IOP (**E,F**); and seven months post-elevated IOP (**G,H**). For each time period these two layers were aligned using blood vessels as landmarks (red arrows). GABAa receptor bands are seen at two (**D**), four (**F**) and seven months (**H**) post-elevated IOP. (**E,G,H**) These sections were slightly oblique; therefore, layer 5 is starting to become evident in certain portions of the sections.

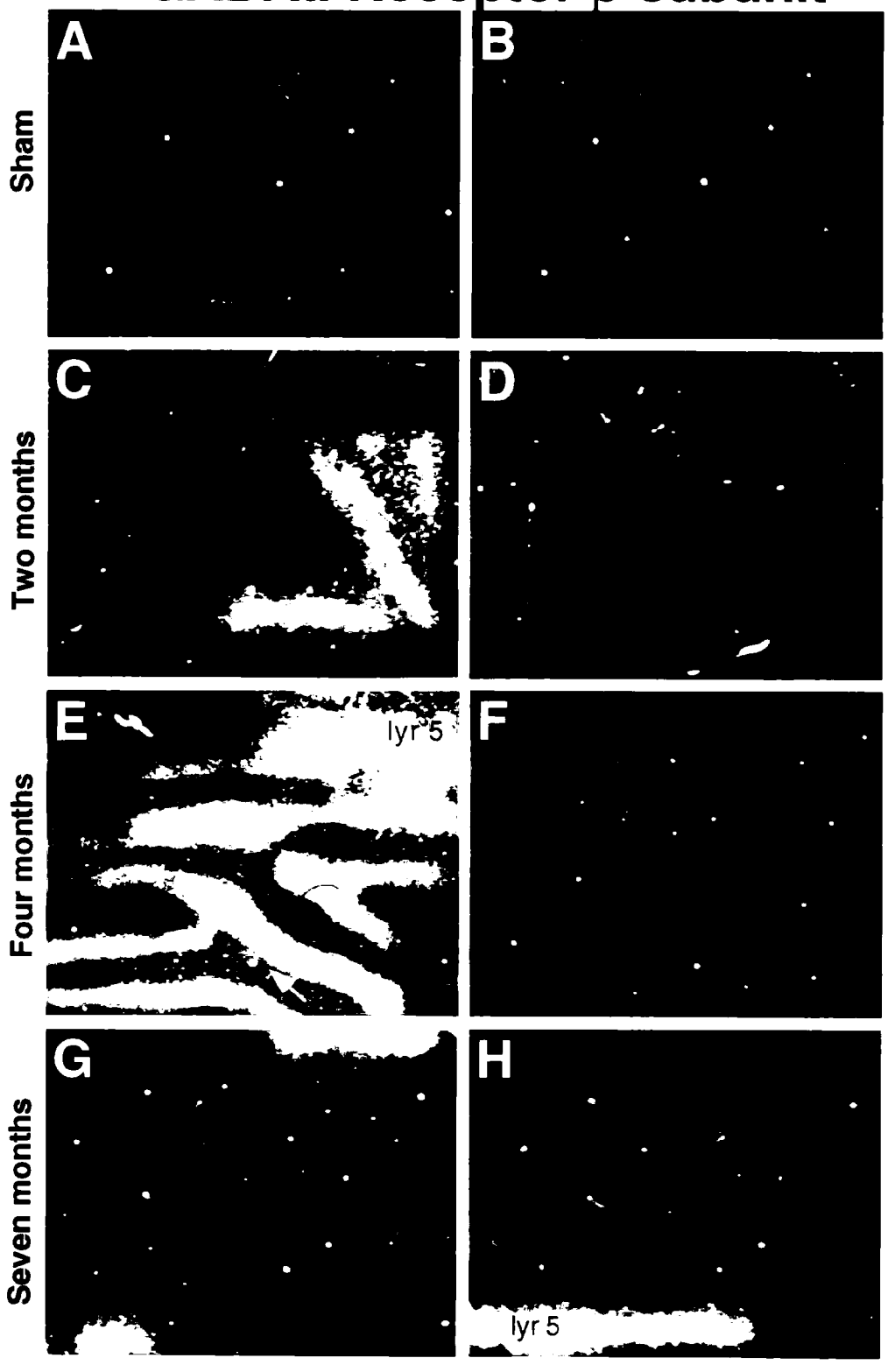
GABAa-Receptor β-subunit
Sham
Two months
Four months
Seven months
A
B
C
D
E
F
G
H
lyr 5
lyr 5

Figure 11: CAMKIIα immunohistochemistry. CO histochemistry in layers 2/3 (**A, C, E, G**) and CAMKIIα immunohistochemistry in layer 4 (**B, D, F, H**). CAMKIIα was reacted on animals who were sham operated (**A,B**), two months post-elevated IOP (**C,D**); four months post-elevated IOP (**E,F**); and seven months post-elevated IOP (**G,H**). For each time period these two layers were aligned using blood vessels as landmarks (red arrows).

Calcium-dependent protein kinase II α

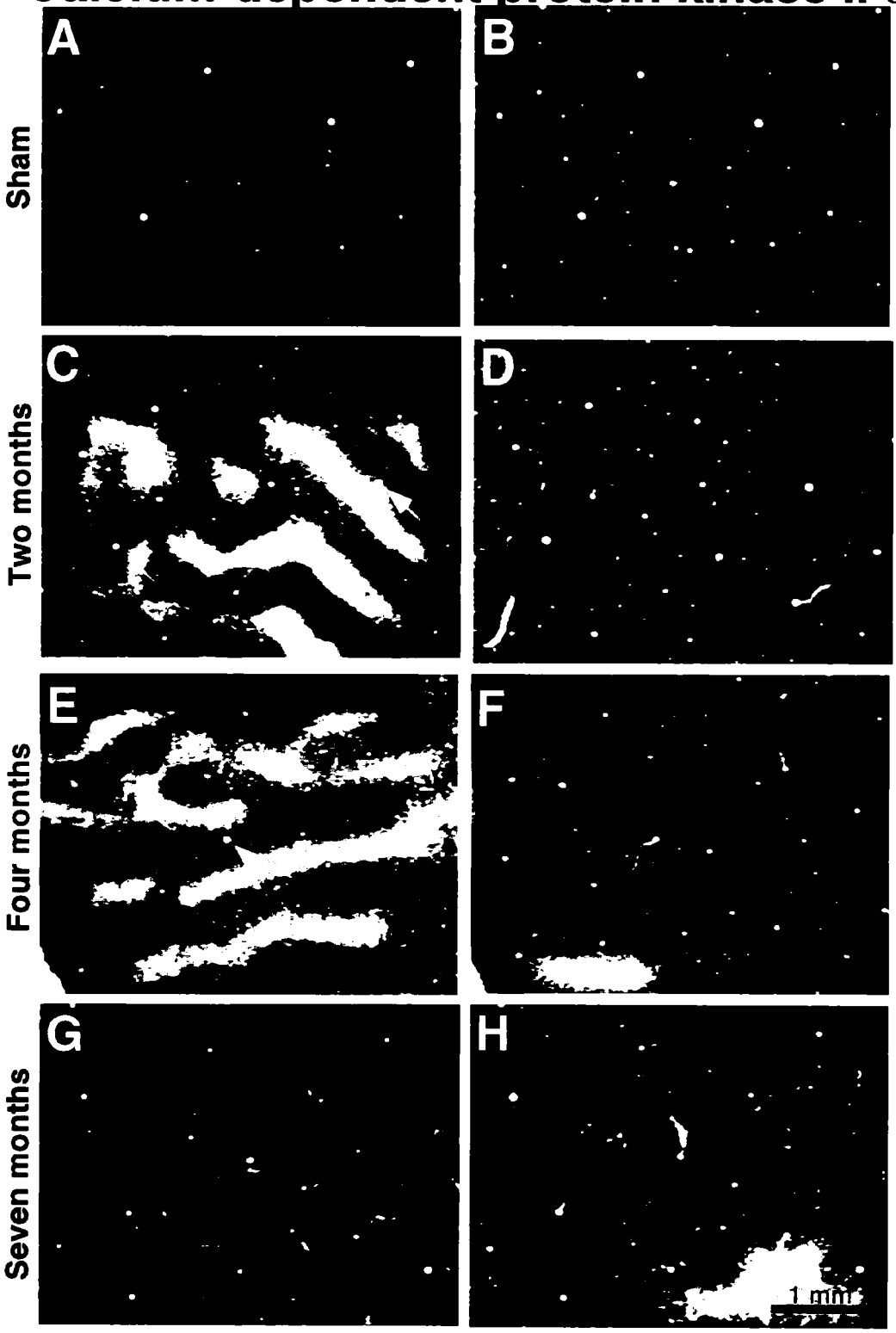

Growth-Associated Protein

At two months post-elevated IOP, differential GAP-43 immunostaining was observed. A pattern of light and dark immunostained GAP-43 bands (Figure 8D) co-aligned with the light and dark CO stained bands (Figure 8C). The light GAP-43 bands were associated with the deprived eye columns and the dark GAP-43 bands were associated with the non-deprived eye columns. The difference in GAP-43 densities between the two eyes was found to be significantly different from each other (0.033 ± 0.001, $p<0.001$) (Figure 8). The ratio of visual:frontal cortex GAP-43 densities was 0.855 ± 0.006 for the non-deprived eye and 0.829 ± 0.005 for the deprived eye (Figure 12). When compared to ratios derived from normal tissues (0.763 ± 0.003), the ratio of GAP-43 density in the glaucomatous tissue was significantly greater than the ratios from normal tissue ($p<0.001$) (Figure 13).

Synaptophysin

Differential staining of SYN in the deprived and non-deprived columns was not observed at this time point (Figure 9D), even though light and dark CO stained bands were visible (Figure 9C).

GABAa Receptor

Immunostaining against the GABAa receptor revealed a pattern of alternating light and dark bands, similar to GAP-43 immunostaining. The light GABAa receptor bands (Figure 10D) corresponded with the deprived eye columns (Figure 10C) and the dark GABAa receptor bands (Figure 10D) corresponded with the non-deprived eye columns (Figure 10C).

The difference in GABAa receptor densities between the two eyes was found to be significantly different from each other (0.047 ± 0.002; $p<0.001$) (Figure 14). The ratio of visual:frontal cortex of GABAa receptor densities was 0.815 ± 0.012 for the non-deprived eye

Figure 12: GAP-43 protein density difference between normal and deprived eye columns of glaucomatous animals. For each deprivation period, the optical density (OD) of GAP-43 immunohistochemistry from the deprived eye was compared to the OD value of the neighboring non-deprived eye. The difference in GAP-43 density between the deprived and non-deprived eye band was determined for two months post elevated IOP (0.031 ± 0.001); four months post-elevated IOP (0.042 ± 0.002) and seven months post-elevated IOP (0.042 ± 0.002).

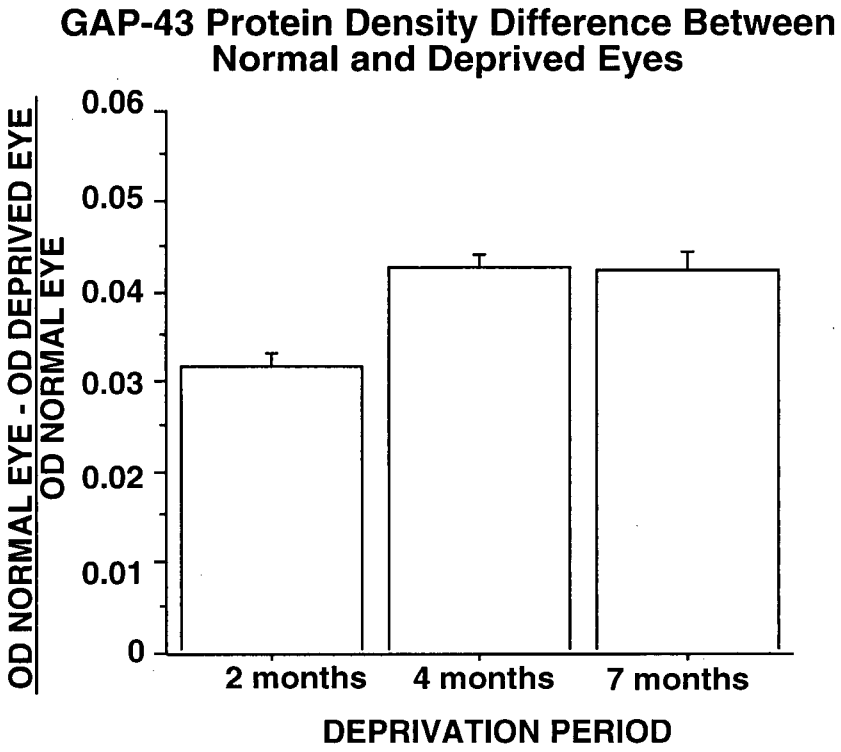
GAP-43 Protein Density Difference Between Normal and Deprived Eyes
OD NORMAL EYE - OD DEPRIVED EYE / OD NORMAL EYE
0.06
0.05
0.04
0.03
0.02
0.01
0
2 months
4 months
7 months
DEPRIVATION PERIOD

Figure 13: GAP-43 protein density in glaucomatous and normal primates. Changes in GAP-43 optical density (OD) ratios were determined by comparing OD between normal animal tissues and glaucomatous tissues. For both normal and glaucomatous animals, visual cortices were 'normalized' using OD values from frontal cortical tissues. In glaucomatous animals, OD values for non-deprived eye columns were normalized to OD values from corresponding frontal cortex (light bars on the graph) and OD values for deprived eye columns were normalized to OD values from corresponding frontal cortex (dark bars on the graph). In normal animals, OD values from layer 4 of the visual cortex was normalized to OD values from corresponding frontal cortex. For all three deprivation periods, OD in for all three deprivation periods were higher than OD in the normal animal. Two months post elevated IOP (0.855 ± 0.006 – non-deprived eye column, 0.829 ± 0.006 – deprived eye column); four months post elevated IOP (0.810 ± 0.004 - non-deprived eye column, 0.778 ± 0.004 - deprived eye column), seven months post elevated IOP (0.843 ± 0.006 - non-deprived eye column, 0.808 ± 0.006 - non-deprived eye column); normal animal 0.85 ± 0.01.

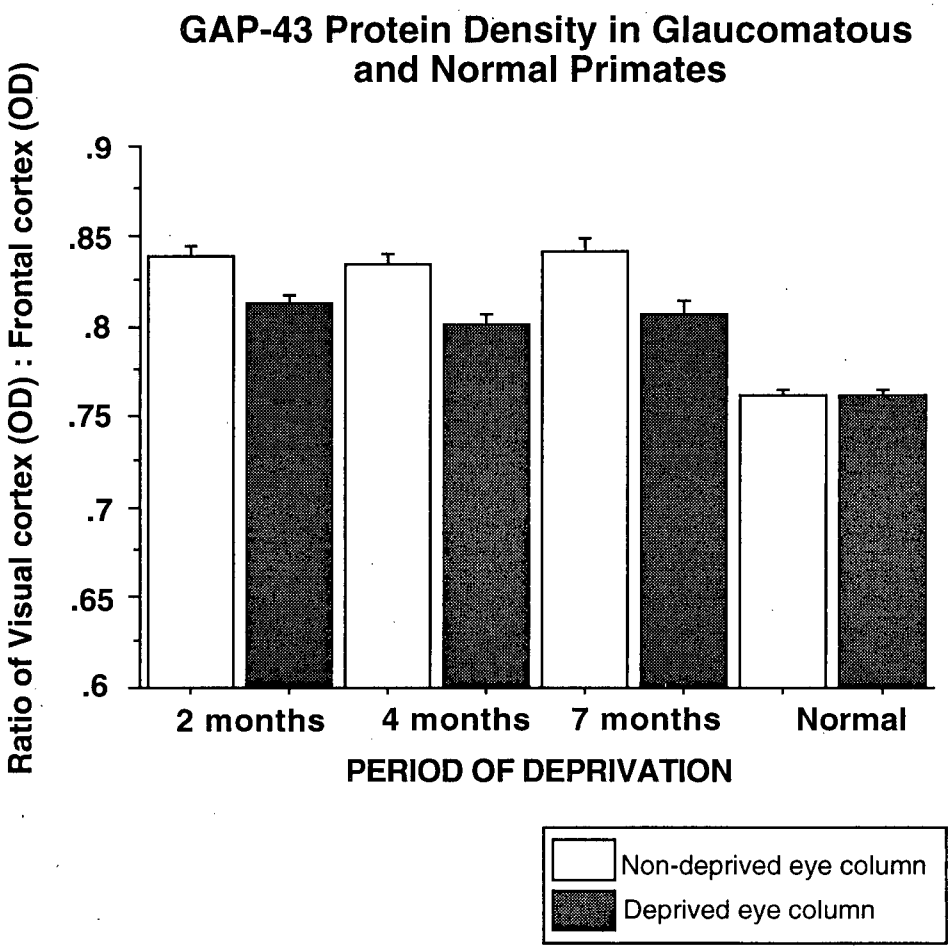
GAP-43 Protein Density in Glaucomatous and Normal Primates
Ratio of Visual cortex (OD) : Frontal cortex (OD)
.9
.85
.8
.75
.7
.65
.6
2 months
4 months
7 months
Normal
PERIOD OF DEPRIVATION
Non-deprived eye column
Deprived eye column

Figure 14: GABAa receptor protein density difference between normal and deprived eye columns of glaucomatous animals. The optical density (OD) of the GABAa receptor immunohistochemistry from the deprived eye column was compared to the OD value of the neighboring non-deprived eye column. The difference in GABAa receptor density between the deprived and non-deprived eye columns was determined for two months post elevated IOP (0.047 ± 0.002); four months post-elevated IOP (0.050 ± 0.005) and seven months post-elevated IOP (0.050 ± 0.003).

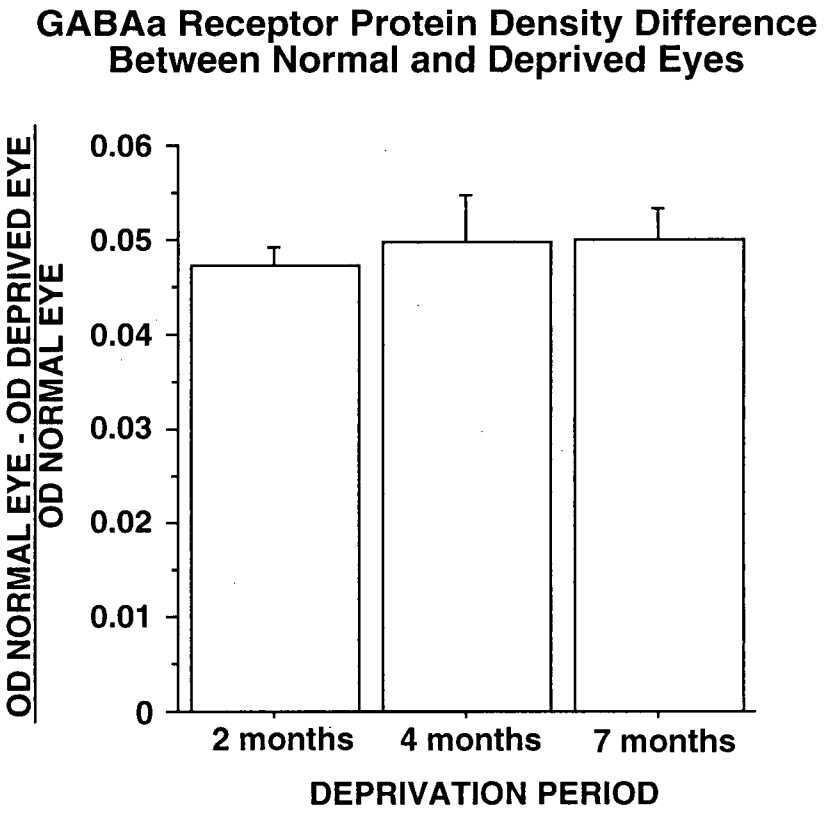
GABAa Receptor Protein Density Difference
Between Normal and Deprived Eyes
OD NORMAL EYE - OD DEPRIVED EYE
OD NORMAL EYE
0.06
0.05
0.04
0.03
0.02
0.01
0
2 months
4 months
7 months
DEPRIVATION PERIOD

and 0.780 ± 0.012 for the deprived eye (Figure 15) and ratios from glaucomatous tissue were found to be significantly less than ratios derived from normal tissue (0.86 ± 0.01; $p<0.001$) .

Calcium-dependent protein kinase IIα

Immunostaining against CAMKIIα revealed a pattern of alternating light and dark bands; however, in contrast to GAP-43 and GABAa receptor immunostaining, the light CAMKIIα bands (Figure 11D) corresponded with the non-deprived eye columns (Figure 11C) and the dark CAMKIIα bands (Figure 11D) corresponded with the deprived eye columns (Figure 11C).

The difference in CAMKIIα densities between the two eyes was found to be significantly different (0.051 ± 0.004; $p<0.001$) (Figure 16). The ratio of visual:frontal cortex CAMKIIα densities was 0.761 ± 0.008 for the non-deprived eye and 0.799 ± 0.008 for the deprived eye (Figure 17). When compared to ratios derived from normal tissue (0.871 ± 0.008), the ratios of CAMKIIα in glaucomatous tissue were significantly less than that of normal tissue ($p<0.001$).

ii. Four Months post-elevated IOP

Cytochrome oxidase

At four months post-elevated IOP the pattern of light and dark CO bands in layer 4C were evident in visual cortex representing both the central and peripheral visual fields (Figure 7F).

In layers 2/3 there were rows of shrunken CO patches alternating with rows of interconnected CO patches (Figure 7E). The rows of shrunken CO patches were located in the centre of light CO bands in layer 4C (Figure 7E, F).

Growth Associated Protein

At four months post-elevated IOP, differential GAP-43 immunostaining was again observed. The pattern of light immunostained GAP-43 bands coaligned with the deprived eye

Figure 15: GABAa receptor protein density in glaucomatous and normal primates. Changes in the GABAa receptor optical density (OD) ratios were determined by comparing OD between normal and glaucomatous animals. OD values for non-deprived eye columns were compared to OD values from corresponding frontal cortex (light bars on the graph) and OD values for deprived eye columns were compared to OD values from corresponding frontal cortex (dark bars on the graph). OD ratios were derived for all three deprivation periods: two months post elevated IOP (0.815 ± 0.012 – non-deprived eye column, 0.780 ± 0.012 – deprived eye column); four months post elevated IOP (0.831 ± 0.006 - non-deprived eye column, 0.793 ± 0.006 - deprived eye column), seven months post elevated IOP (0.775 ± 0.008 - non-deprived eye column, 0.736 ± 0.009 - non-deprived eye column). OD values from experimental animals were compared to normal (non-deprived) animals 0.736 ± 0.009.

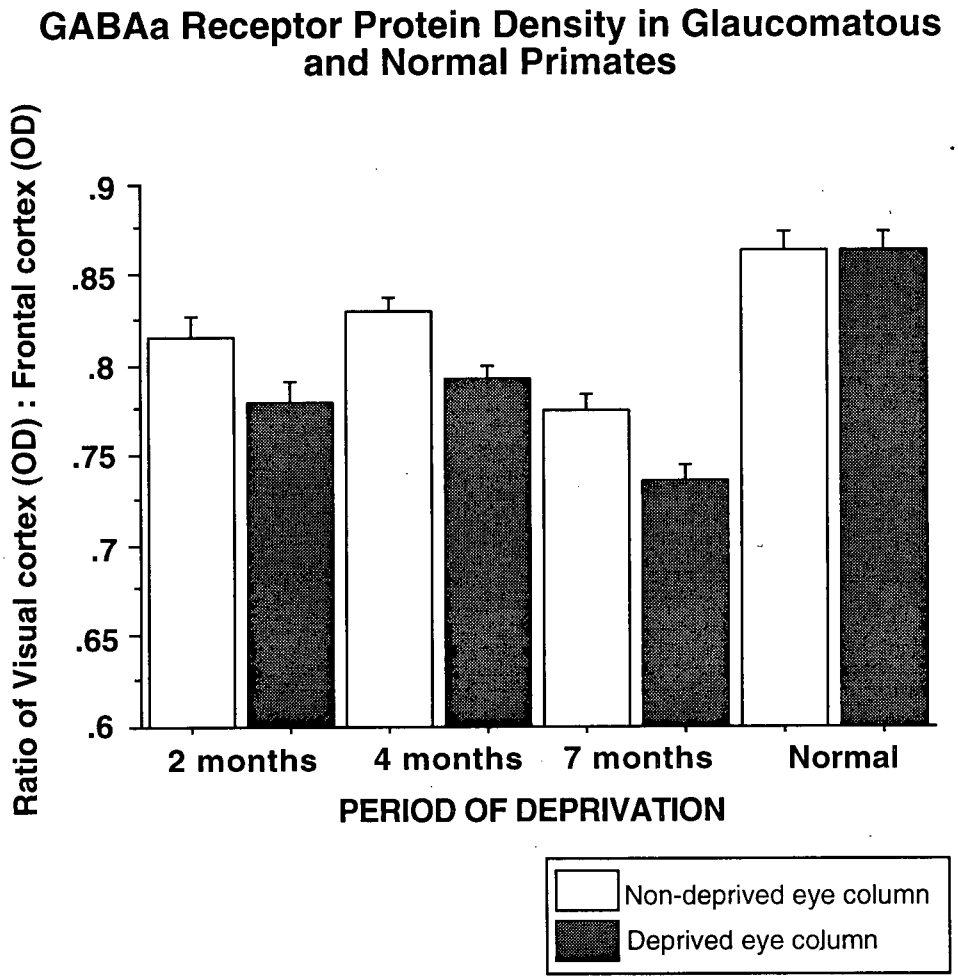
GABAa Receptor Protein Density in Glaucomatous and Normal Primates
Ratio of Visual cortex (OD) : Frontal cortex (OD)
.9
.85
.8
.75
.7
.65
.6
2 months
4 months
7 months
Normal
PERIOD OF DEPRIVATION
Non-deprived eye column
Deprived eye column

Figure 16: CAMKIIα protein density difference between normal and deprived eye columns of glaucomatous animals. The optical density (OD) of CAMKIIα immunohistochemistry from the deprived eye columns was compared to the OD value of the neighboring non-deprived eye columns. The difference in CAMKIIα density between the deprived and non-deprived eye columns was determined for two months post elevated IOP (0.051 ± 0.004); four months post-elevated IOP (0.051 ± 0.002) and seven months post-elevated IOP (0.072 ± 0.004).

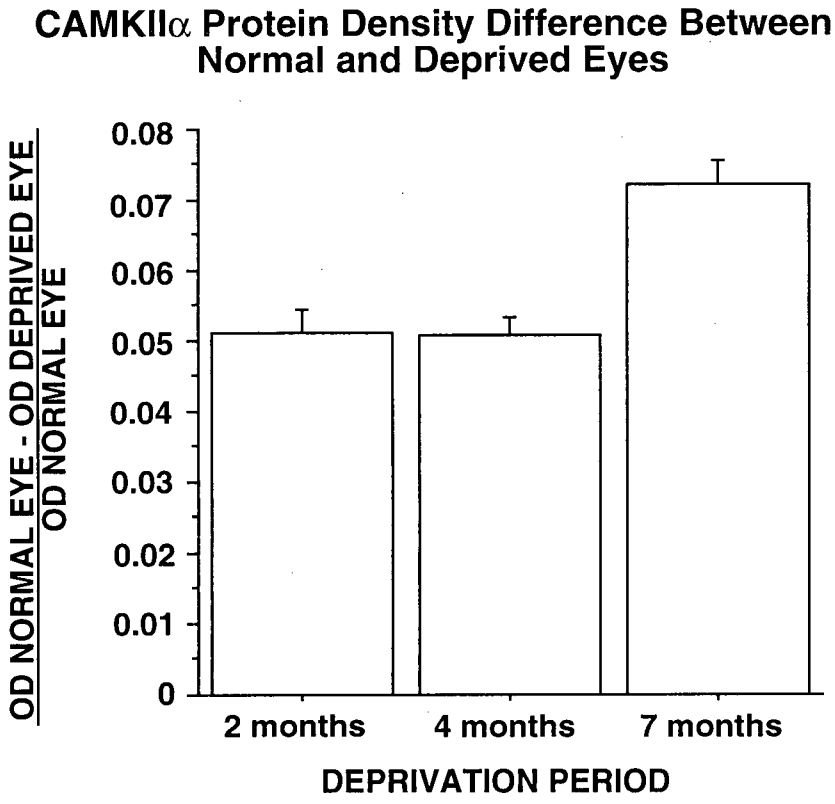
CAMKIIα Protein Density Difference Between Normal and Deprived Eyes
OD NORMAL EYE - OD DEPRIVED EYE / OD NORMAL EYE
0.08
0.07
0.06
0.05
0.04
0.03
0.02
0.01
0
2 months
4 months
7 months
DEPRIVATION PERIOD

Figure 17: CAMKIIα protein density in glaucomatous and normal primates. Changes in CAMKIIα optical density (OD) ratios were determined by comparing OD between normal and glaucomatous animals. OD values for non-deprived eye columns were compared to OD values from corresponding frontal cortex (light bars on the graph) and OD values for deprived eye columns were compared to OD values from corresponding frontal cortex (bars on the graph). OD ratios were derived for all three deprivation periods: two months post elevated IOP (0.761 ± 0.008 – non-deprived eye column, 0.799 ± 0.008 – deprived eye column); four months post elevated IOP (0.767 ± 0.006 - non-deprived eye column, 0.805 ± 0.006 - deprived eye column), seven months post elevated IOP (0.688 ± 0.008 - non-deprived eye column, 0.737 ± 0.008 - non-deprived eye column). OD values from experimental animals were compared to normal (non-deprived) animals 0.835 ± 0.011.

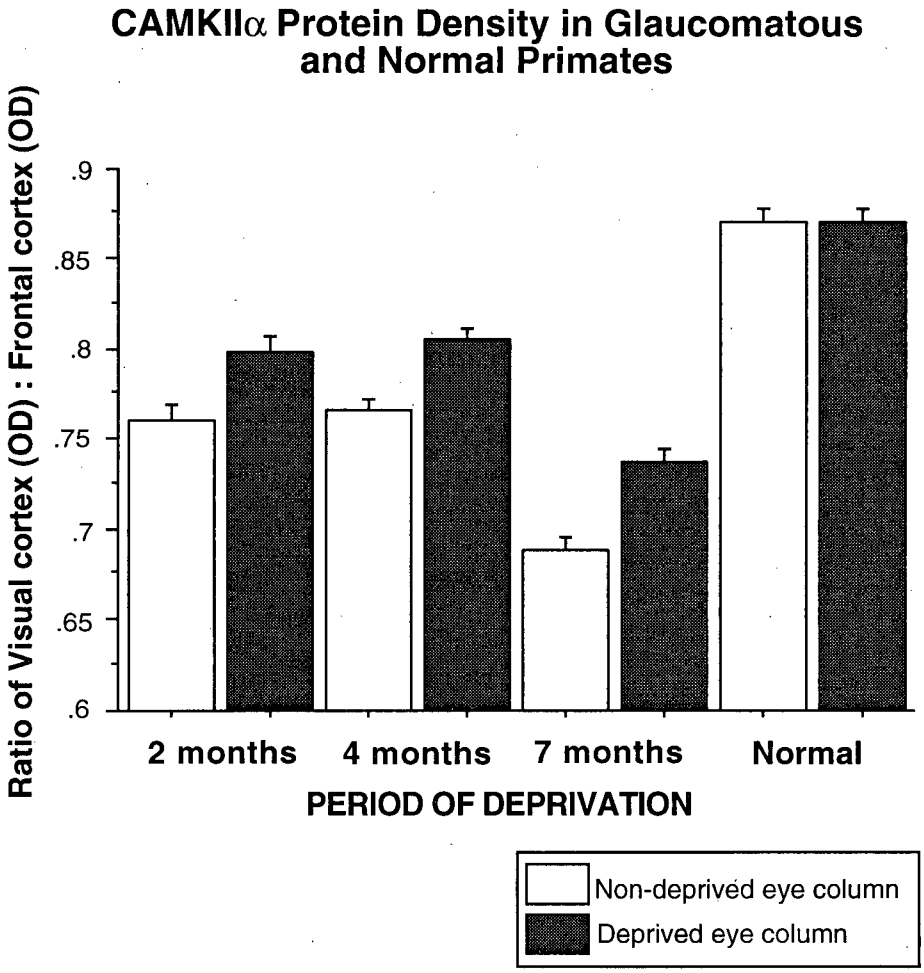
CAMKIIα Protein Density in Glaucomatous and Normal Primates
Ratio of Visual cortex (OD) : Frontal cortex (OD)
.9
.85
.8
.75
.7
.65
.6
2 months
4 months
7 months
Normal
PERIOD OF DEPRIVATION
Non-deprived eye column
Deprived eye column

columns and the dark GAP-43 bands co-aligned with the non-deprived eye columns (Figure 8E,F). The difference in GAP-43 density between the two eyes was also found to be significantly different (0.042 ± 0.002; $p<0.001$) (Figure 12). The ratio of visual:frontal cortex for GAP-43 density was 0.810 ± 0.004 for the non-deprived eye and 0.778 ± 0.004 for the deprived eye (Figure 13). When compared to GAP-43 density ratios from normal animals (0.763 ± 0.003), GAP-43 levels in both eye columns of glaucomatous animals were significantly greater than normal animals ($p<0.001$).

Synaptophysin

Differential staining in SYN between the deprived and non-deprived eye columns was observed in layer 4C at four months post-elevated IOP (Figure 9E, F). The dark SYN bands coaligned with the dark CO bands (non-deprived eye) and the light SYN bands coaligned with the light CO bands (deprived eye).

Optical density measurements of SYN immunostaining between the deprived and non-deprived eye were significantly different (0.045 ± 0.002; $p<0.001$) (Figure 18). The ratio of visual:frontal cortex for SYN densities in the non-deprived eye of glaucomatous tissue (0.896 ± 0.009) was significantly greater than ratios derived from normal tissue($p<0.001$) (Figure 19). However, the ratio of visual:frontal cortex for SYN densities in the deprived eye columns of glaucomatous tissue (0.856 ± 0.008) was not significantly different from ratios derived from normal tissue (0.875 ± 0.007; $p<0.001$) (Figure 19).

GABAa Receptor

Similar to GAP-43 and SYN immunostaining, at four months post-elevated IOP, differential GABAa receptor immunostaining was observed and light and dark immunostained GABAa receptor bands coaligned with the light and dark CO stained bands respectively (Figure 10E, F). The difference in GABAa receptor density between the two eyes was significantly

Figure 18: SYN protein density difference between normal and deprived eye columns of glaucomatous animals. The optical density (OD) of SYN immunohistochemistry from the deprived eye columns was compared to the OD value of the neighboring non-deprived eye columns. The difference in SYN density between the deprived and non-deprived eye columns was only determined for the four months post-elevated IOP (0.045 ± 0.002) deprivation period.

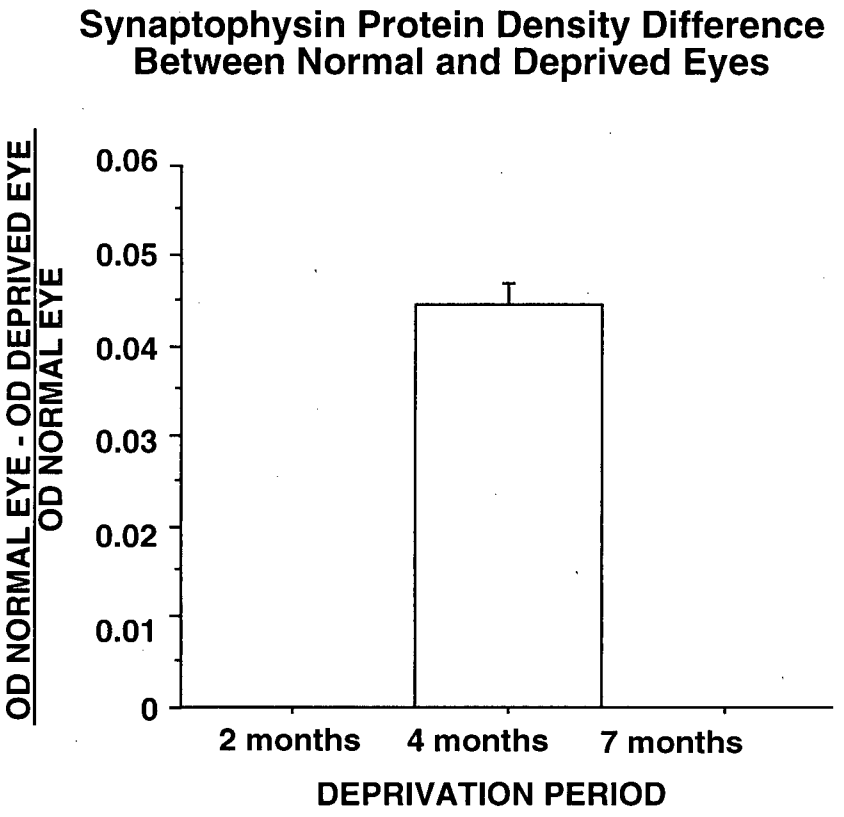
Synaptophysin Protein Density Difference
Between Normal and Deprived Eyes
OD NORMAL EYE - OD DEPRIVED EYE
OD NORMAL EYE
0.06
0.05
0.04
0.03
0.02
0.01
0
2 months
4 months
7 months
DEPRIVATION PERIOD

Figure 19: SYN protein density in glaucomatous and normal primates. Changes in SYN optical density ratios were determined by comparing optical densities between normal and glaucomatous animals. OD values for non-deprived eye columns were compared to OD values from corresponding frontal cortex (light bars on the graph) and OD values for deprived eye columns were compared to OD values from corresponding frontal cortex (bars on the graph). OD ratios were compared between four months post elevated IOP (0.896 ± 0.009 - non-deprived eye column, 0.856 ± 0.008 - deprived eye column) to normal (non-deprived) animals 0.875 ± 0.007.

SYN Protein Density in Glaucomatous and Normal Primates

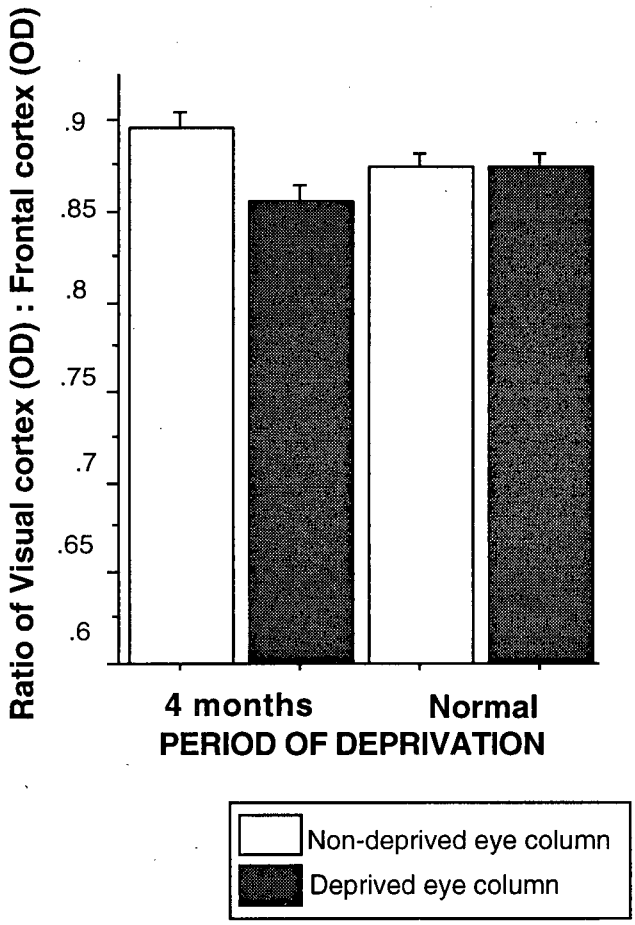

different (0.050 ± 0.005; $p<0.001$) (Figure 14). The ratio of visual:frontal cortex of GABAa receptor density of glaucomatous tissue for the non-deprived eye (0.831 ± 0.006) and for the deprived eye (0.793 ± 0.006) was significantly less than ratios derived from normal tissue (0.86 ± 0.01; $p<0.001$) (Figure 15).

Calcium-dependent protein kinase IIα

The complementary CAMKIIα pattern to CO staining seen at 2 months was also observed at four months post-elevated IOP (Figure 11E, F). Immunostaining against CAMKIIα revealed a pattern of alternating light and dark bands which corresponded with the non-deprived eye and deprived eye columns, respectively.

The difference in CAMKIIα density between the two eyes was again observed to be significantly different (0.051 ± 0.002; $p<0.001$) (Figure 16). The ratio of visual:frontal cortex of CAMKIIα density derived from non-deprived (0.767 ± 0.006) and deprived eye columns (0.805 ± 0.006) of glaucomatous tissue was significantly different from ratios derived from normal tissue (0.871 ± 0.008; $p<0.001$) (Figure 17).

iii. Seven Months post-elevated IOP

Cytochrome oxidase

The CO patterns in layers 4C and 2/3 were similar to other animals at earlier deprivation periods (Figure 7G, H).

Growth Associated Protein-43:

The GAP-43 immunostaining pattern at seven months post-elevated IOP was similar to that seen at the two and four months deprivation times (Figure 8G, H). Bands were seen in both the peripheral and central visual field representations and the difference in GAP-43 density between the two eyes was significantly different from each other (0.042 ± 0.001; $p<0.001$) (Figure 12). The ratios of visual:frontal cortex of GAP-43 density of glaucomatous animal's non-

deprived eye bands (0.843 ± 0.008) and deprived eye bands (0.808 ± 0.006) were significantly greater than ratios derived from normal animals (0.763 ± 0.003; $p<0.001$) (Figure 13)

Synaptophysin:

Differential staining of SYN in the deprived and non-deprived columns was not observed at seven months post elevated IOP (Figure 9G, H).

GABAa receptor

Differential immunostaining of the GABAa receptor continued through to seven months post-elevated IOP where the dark and light bands coaligned with the dark CO bands of the normal eye and the light CO bands of the deprived eye, respectively (Figure 10G, H). The ratio of visual:frontal cortex of GABAa receptor density in the deprived eye (0.736 ± 0.009) and the non-deprived eye (0.86 ± 0.01) of glaucomatous tissue were significantly different from ratios of GABAa receptor density found in normal tissues (0.86 ± 0.01; $p<0.001$) (Figure 15).

Calcium-dependent protein kinase IIα

The complementary CAMKIIα pattern to CO staining was again observed at seven months post-elevated IOP. Immunostaining against CAMKIIα revealed a pattern of alternating light and dark bands which corresponded with the non-deprived eye and deprived eye columns respectively (Figure 11G, H).

The difference in CAMKIIα density between the two eyes was again observed to be significantly different from each other (0.072 ± 0.004; $p<0.001$) (Figure 16). The ratio of CAMKIIα in the visual:frontal cortex of non-deprived eye (0.688 ± 0.008) and of deprived eye (0.737 ± 0.008) bands from glaucomatous tissue was significantly less than ratios derived from normal tissues (0.871 ± 0.008; $p<0.001$) (Figure 17).

C. Experimental animals – Intra-animal Comparisons

The difference in GAP-43 density between the two eyes at 4 and 7 months post-elevated IOP was significantly greater than the difference in GAP-43 density between the two eyes at two months post-elevated IOP; $p<0.001$ (Figure 12). It appears that the difference in GAP-43 density begins to plateau at 4 months post-elevated IOP and continues through to 7 months post-elevated IOP. On the other hand, differences in GABAa receptor density between the two eyes was not significantly different across the three deprivation periods ($p<0.001$) (2, 4, and 7 months post elevated IOP) (Figure 14). CAMKIIα density, between the two eyes, at two and four months post-elevated IOP was significantly less than the difference in CAMKIIα density found at seven months post-elevated IOP ($p<0.001$) (Figure 16). Again, similar to what is seen in GAP-43, the difference in CAMKIIα density between the two eyes is greater at the longer deprivation period ($p<0.001$) (7 months post elevated IOP)

4. Discussion

In this study we analyzed two possible consequences of elevated IOP. One was the differences in protein densities found in the visual cortices of experimental animals versus the visual cortices of normal animals (inter-animal comparison). The second was the difference in protein densities between deprived and non-deprived eye columns of glaucomatous animals over three deprivation periods (intra-animal comparison).

A. Inter-animal

The plasticity markers, GAP-43, SYN, GABAa receptor and CAMKIIα demonstrated small, but significant changes in protein density between glaucomatous and normal animals. In our experiment, we saw an overall increase in GAP-43 and SYN protein density in glaucomatous animals suggesting that there could be axonal growth as a result of elevated IOP. Our results also show an overall decrease of the GABAa receptor and CAMKIIα protein densities in

glaucomatous animals, suggesting a decrease in inhibition and a possible mechanism to counterbalance the synaptic and axonal growth that is occurring in response to the deprivation.

i. Upregulation of neurochemicals:

Knowing that levels of GAP-43 are normally very low in the adult visual cortex (Nelson et al 1987), and the propensity for GAP-43 to increase after axotomy (Doster et al 1991, Skene JHP and Willard M 1981a), we would have predicted an increase in GAP-43 only in deprived eye columns; however, we found an increase in GAP-43 in both deprived and non-deprived eye columns. It is possible that soon after deprivation, there was an increase of GAP-43 only in the deprived eye columns and that our shortest deprivation period of two months post-elevated IOP was not short enough to observe this. Because the expression of GAP-43 protein, is found in the axon terminals of neurons (Chong et al 1994; Linda et al 1992; McNeill et al 1999; Tetzlaff et al 1991) and also found in the neuropil surrounding neurons (Liu and Jones 1996), the increased levels of GAP-43 found in non-deprived eye columns are likely due to neurons within these columns and not as a result of sprouting from neighboring columns.

At all three deprivation periods, GAP-43 density was increased in glaucomatous animals when compared to normal animals. The fact that both cortical columns appear to be upregulated in GAP-43 protein suggests axonal growth occurring throughout layer 4C of area 17. This is supported by other studies involving cortical expansion, sprouting of axon collaterals and synaptogenesis (Darian-Smith and Gilbert 1994, 1995; Gilbert and Wiesel 1992; Heinen and Skavenski 1991; Kaas et al 1990) which have shown that functional rearrangement can occur in the visual cortex after peripheral deafferentation.

While GAP-43 was upregulated for all three deprivation periods, SYN was only upregulated at the four month deprivation period in the non-deprived eye columns. Indicating that the levels of SYN immunoreactivity appear to change independently of GAP-43

immunoreactivity. This suggests that levels of SYN density may only be occurring during a particular time post-deprivation. Deafferentation in the dentate gyrus of the hippocampus results in changes of GAP-43 immunoreactivity before changes in SYN immmunoreactivity (Masliah et al 1991), we predict that axons need to sprout or branch first (signals from GAP-43) and once the pre-synaptic terminals of these branches are stable, synapses form.

ii. Downregulation of neurochemicals:

Both CAMKIIα and GABAa receptor densities were downregulated in the visual cortices of glaucomatous animals. In this study, a decrease of GABAa receptor density was found in area VI of glaucomatous animals as compared to normal animals. Given that the GABAa receptor is involved in inhibitory transmission throughout the CNS (Bowery 1983; Johnston et al 1984), this decrease in GABAa receptor suggests a decrease in inhibitory transmission in response to elevated IOP. This is similar to previous reports (Hendry et al 1994; Hendry and Jones 1986; 1988) where GABAa receptor and GABAergic neurons are found to decrease following a reduction in visual activity.

Hendry et al 1994 reported that simultaneous processing of normal and monocularly deprived visual cortices produced immunostaining in the normal monkey to be 'similar in intensity to the immunostaining of normal-eye columns'. Our study demonstrates that GABAa receptor protein density was always greater in non-deprived eye columns than in deprived eye columns even though both eye columns stained for less protein than normal animals. Their study examined deprivation periods for a maximum period of 30 days, whereas our shortest deprivation period was for two months. We would predict that at a shorter duration of elevated IOP, we would see the density of GABAa receptors downregulated only in the deprived eye columns. GABAa receptor is regulated by visual activity (Hendry et al 1990) which accounts for the fact

that its protein density is consistently greater in non-deprived eye bands than the deprived eye columns, even though both are downregulated from normal animals.

Although monocular deprivation results in a reduction of immunoreactive GABA, the fact that this reduction in the neurotransmitter level can be reversed following the return of binocular vision (Hendry and Jones 1988) suggests that the deprivation is not accompanied by cortical death of GABA cells. Given that GAP-43 is upregulated while GABAa receptors are downregulated, removal of inhibition in the visual cortex is allowing axonal growth to occur in area VI.

Similar to the GABAa receptor densities, CAMKIIα densities were downregulated in the glaucomatous animals as compared to the normal animals. There is an overall downregulation of the kinase in glaucomatous animals as compared to normal animals. CAMKIIα may play a role in synaptic function or synaptic efficacy based on its presence in presynaptic terminals (Ouimet et al 1984), its involvement in the regulation of transmitter release (Llinas et al 1985) and its association with postsynaptic densities (Miller and Kennedy 1985). The reduction in CAMKIIα levels suggests that there is a reduction in synaptic function which might appear puzzling since there are increased levels of GAP-43 and SYN; however, CAMKIIα could be serving to control the numbers and or types of synapses and in effect act as a counterbalance to GAP-43 and SYN levels.

B. Intra-animal

Our results show that protein levels do differ between deprived and non-deprived eye columns of experimental animals. This difference yielded dark and light immunostained bands, which corresponded with ocular dominance bands stained with CO. GAP-43, SYN and GABAa receptor protein densities were found to be greater in the non-deprived eye bands, whereas CAMKIIα protein density was found to be greater in the deprived eye bands. Although light and

dark immunostained bands were found at all three deprivation periods for GAP-43, GABAa receptor and CAMKIIα protein, SYN immunostained bands were only observed at the 4 month deprivation period.

While examining the differences in protein densities between the deprived and non-deprived eye bands, GABAa receptor protein densities remained the same throughout the three deprivation periods, suggesting that levels of inhibition between the two eye bands were not fluctuating. However, GAP-43 and CAMKIIα demonstrated greater differences in protein densities at the longer deprivation periods (four and seven months post-elevated IOP), suggesting one of three possibilities occurring. One, protein densities for GAP-43 in deprived eye bands are decreasing; two, protein densities are increasing in the non-deprived eye bands or three, protein densities are decreasing in deprived eye bands and increasing in non-deprived eye bands. Similar assumptions can be made for CAMKIIα with the exception that increasing protein densities would be occurring in deprived eye bands and decreasing protein densities would be occurring in non-deprived eye bands.

Since the levels of GAP-43 is normally low in adult cortex (Nelson et al 1987) it is unlikely that the deprived eye columns are further reducing their GAP-43 protein densities; therefore, GAP-43 protein densities must be increasing in the non-deprived eye bands suggesting once again that cortical activity is driving the expression of this protein. Although there is an overall increase of GAP-43 levels in glaucomatous cortices, we speculate that GAP-43 levels are greater in non-deprived eye bands because it is receiving more cortical activity. Unilateral increase in IOP, similar to monocular deprivation, decreases the level of visual activity in the deprived eye (Crawford 2000, Wong-Riley et al 1989); therefore, the cortical activity that the non-deprived eye is receiving plays a role in the regulation of GAP-43 levels.

CAMKIIα levels are found to be upregulated when neural activity is reduced (Benson et al 1991a, 1991b, 1992; Hendry and Kennedy 1986) therefore the likely scenario is that when subjected to longer deprivation periods, CAMKIIα protein density increases in the deprived eye bands. Upregulation of CAMKIIα when neural activity is reduced (Benson et al 1991a; Hendry and Kennedy 1986) and downregulation of CAMKIIα when activity is increased (Bronstein et al 1992; Liang and Jones 1997; Murray et al 1995;) may explain why deprived eye columns are more densely immunostained for CAMKIIα than non-deprived eye columns.

In regards to the differences in GABAa receptor protein densities, either there are no changes in GABAa receptor protein levels or the increase in protein density in the non-deprived eye bands are occurring simultaneously with decreases in protein density in the deprived eye bands. Nevertheless, the difference between the two eye bands remains the same suggesting that neither eye band gains or loses inhibition more than the other.

Clearly, the differential distribution of neurochemicals is fairly complex. GAP-43 is increased in the non-deprived eye bands, CAMKIIα is increased in the deprived eye bands and SYN isn't even observed to be differentially expressed between the two eye bands until four months post-elevated IOP.

C. Limitations to the study

There were assumptions which need to be addressed. First, the interanimal results are based on assumptions that immunoreactivity of frontal cortex remains constant in spite of elevated IOP. While it is known frontal cortex does play a role in frontal eye fields and saccade movements of the eye, there is no evidence that sensory deprivation results in changes in frontal cortex of the neurochemicals studied here, or of any other neurotransmitter or neuromodulatory proteins. Thus we assumed that levels of expressed proteins remained constant in frontal cortex. Furthermore, our results revealed an apparent downregulation in two proteins (GABAa receptor

and CAMKIIα), while another two (GAP-43 and SYN) demonstrated an apparent upregulation after elevated IOP. Suggesting that any changes in protein densities are due to regulatory mechanisms and that the findings in this study are not artifactual.

Second, intra-animal results revealed small, but significant differences in optical density of immunoreactivity. Differences of approximately 3-7 % between deprived and non-deprived eye bands were seen in this study. Given that overall quantities of GAP-43, SYN, GABAa receptor and CAMKIIα are low in adult visual cortex (Baekelandt 1994, Nelson et al 1987), changes on the scale of that seen here are likely to indeed have some functional impact. Future studies may help clarify whether the immunohistochemical procedures used here in this study underestimate the quantities of expressed proteins or whether in vivo neurons are sensitive enough to such changes in protein levels.

Third, on a technical note, our antibodies were not tested in our lab for animal specificity; therefore, there was the chance that the results from our immunohistochemistry were non-specific. The chance that the results might reflect this is small since in one instance we had deprived eye bands darkly immunostained and in other instances we had deprived eye bands lightly immunostained. This demonstrates that the antibodies were not randomly binding onto the primate tissue. As well, during the preparation of the cortex for shipping to UBC and during histology preparation, shrinkage may be a factor which contributed to our results. If shrinkage was a factor, then this would affect our intra-animal comparisons the most because the numbers are so small. A significant enough shrinkage might make one believe that the differences in protein density between the two eye bands to be negligible; however, differences were found for almost all neurochemical markers at each deprivation period and it is unlikely that enough shrinkage occurred in all cortices to account for our results.

D. Conclusions from our experimental primate model

This study of glaucoma in a primate model has revealed changes in the spatial and temporal distribution of neurochemical markers in the visual cortex. Unilateral elevated IOP results in:

- Differential staining of cytochrome oxidase in layer 4C of the visual cortex.
- A reduction in CO activity two months post-elevated IOP up through to 7 months post-elevated IOP.
- The immunostaining patterns of CAMKIIα reveal that monocular deprivation by elevated IOP does not randomly cause a downregulation of neurochemical markers in the deprived eye bands.
- Immunohistochemical levels of GAP-43 and SYN increase while GABAa receptor and CAMKIIα levels decrease in response to elevated IOP
- The time course of change is specific for each neurochemical, differential GAP-43, GABAa receptor and CAMKIIα staining are observed as early as two months post-elevated IOP; however, SYN is not observed until four months post-elevated IOP and it's an increase in only the non-deprived eye column.

The difference in protein density (GAP-43, SYN, CAMKIIα and GABAa receptor) between the eye bands increased at different times demonstrating the complex nature of cortical reorganization. Cortical reorganization/cortical plasticity is the ability of the cortex to modulate or change its function after peripheral sensory deafferentation. Neurochemical changes found in the adult visual cortex post-elevated IOP involves an overall decrease of inhibition (GABAa receptor) and potential axonal growth and syanptogenesis (GAP-43 and SYN), which could be regulated through intracellular mechanisms (CAMKIIα). Clearly, neurochemicals are tightly regulated in the cortex, and an increase in one marker is not an indicator that all neurochemicals

will increase. Perhaps with elevated IOP a reduction in cortical inhibition allows presynaptic terminals need to become stable until newly synthesized synaptic vesicles are formed and all of which is controlled at the cellular level. Future studies will be needed to elucidate these and other complex neuronal signals mediating cortical plasticity in adult brain.

References

1. Alvarado J, Murphy C, Juster R. Trabecular meshwork cellularity in primary open-angle glaucoma and nonglaucomatous normals. Ophthalmology. 1984; 91(6):564-579.

2. Anderson DR, Hendrickson A. Effect of intraocular pressure on rapid axoplasmic transport in monkey optic nerve. Investiagive Ophthalmology. 1974;13:771-783.

3. Araie M, Sekine M, Suzuki Y, Koseki N. Factors contributing to the progression of visual field damage in eyes with normal-tension glaucoma. Ophthalmology. 1994; 101(8):1440-1444.

4. Armaly MF. The genetic determination of ocular pressure in the normal eye. Arch Ophthalmol. 1967;78:187-192

5. Armaly MF. Ocular pressure and aqueous outflow facility in siblings. Arch Ophthalmol. 1968;80:354-360.

6. Baekelandt V, Arckens L, Annaert W, Eysel UT, Orban GA, Vandesande F. Alterations in GAP-43 and Synapsin immunoreactivity provide evidence for synaptic reorganzation in adult cat dorsal lateral geniculate nucleus following retinal lesions. Europ J Neurosci. 1994;6:754-765.

7. Baekleandt V, Eysel UT, Orban GA, Vandesande F. Long-term effects of retinal lesions on growth-associated protein 43 (GAP-43) expression in the visual system of adult cats. J Neurosci Lett. 1996;208:113-116.

8. Basi GS, Jacobson RD, Virag I, Schilling J. Skene JH. Primary structure and transcriptional regulation of GAP-43, a protein associated with nerve growth. Cell. 1987;49(6):785-791.

9. Benevento LA, Rezak M. The cortical projections of the inferior pulvinar and adjacent lateral pulvinar in the rhesus monkey (Macaca mulatta): an autoradiographic study. Brain Res. 1976;108(1):1-24.

10. Bennet MK, Erondu NE, Kennedy MB. Purification and characterization of a calmodulin-dependent protein kinase that is highly concentrated in brain. J Biol Chem. 1983;258:127-135.

11. Benowitz LI, Lewis ER. Increased transport of 44,000-49,000 dalton acidic proteins during regeneration of the goldfish optic nerve: a two dimensional gel analysis. J Neurosci. 1983;3:2153-2163.

12. Benowitz LI, Apostolides PJ, Perrone-Bizzozero N, Finklestein SP, Zwiers H. Anatomical distribution of the growth-associated protein GAP-43/B-50 in the adult rat brain. J Neurosci. 1988;8:339-352.

13. Benowitz LI, Perrone-Bizzozero N, Finkelstein SP, Bird ED. Localization of the growth-associated phosphoprotein GAP-43 (B-50, F1) in the human cerebral cortex. J Neurosci. 1989;9:990-995.

14. Benson DL, Isackson PJ, Gall CM, Jones EG. Differential effects of monocular deprivation on glutamic acid decarboxylase and type II calcium-calmodulin-dependent protein kinase gene expression in the adult monkey visual cortex. 1991a;11:31-47.

15. Benson DL, Isackson PJ, Hendry SHC, Jones EG. Differential gene expression for glutamic acid decarboxylase and type II calcium-calmodulin-dependent protein kinase in basal ganglia, thalamus, and hypothalamus of the monkey. J Neurosci. 1991b;11:1540-1564.

16. Benson DL, Isackson PJ, Gall CM, Jones EG. Contrasting patterns in the localization of glutamic acid decarboxylase and Ca/calmodulin protein kinase gene expression in the rat central nervous system. Neuroscience 1992;46:825-850.

17. Bhargava SK, Leighton DA, Phillips CI. Early angle-closure glaucoma. Distribution of iridotrabecular contact and response to pilocarpine. Arch Ophthalmol. 1973;89(5):369-372.

18. Biffo S, Verhaagen J, Schrama LH, Schotman P, Danho W, Margolis FL. B-50/GAP43 expression correlates with process outgrowth in the embryonic mouse nervous system. 1990;2:487-499.

19. Bloom FE. 1985. CNS Plasticity: A survey of opportunities. In: Bignami A, BloomFE, Bolis CL, Adeloy A (eds) Central Nervous Syste Plasticity and Repair. Raven Press, New York p3-11.

20. Bowery NG, Classification of GABA receptors. In: The GABA receptors. Enna SJ, ed. 1983. p177-213 Clifton, NJ.

21. Boyd J, Matsubara J. Laminar and columnar patterns of geniculocortical projections in the cat: relationship to cytochrome oxidase. J Comp Neurol. 1996;19;365(4):659-682.

22. Brock To, O'Callaghan JP. Quantitative changes in the synaptic vesicle proteins synapsin I and p38 and the astrocyte-specific protein glial fibrillary acidic protein are associated with chemical-induced injury to the rat central nervous system. J Neurosci. 1987;7(4):931-942.

23. Bronstein JM, Micevych P, Popper P, Huez G, Farber DB, Wasterlain CG. Long-lasting decreases of type II calmodulin kinase expression in kindled rat brains. Brain Res. 1992 Jul 3;584(1-2):257-260.

24. Buckley KM, Floor E, Kelly RB. Cloning and sequence analysis of cDNA encoding p38, a major synaptic vesicle protein. J Cell Biol. 1987;105(6 Pt 1):2447-2456.

25. Bulleit RF, Bennett MK, Malloy SS, Hurley JB, Kennedy MB. Conserved and variable regions in the subunits of brain type II Ca2+/calmodulin dependent protein kinase. Neuron. 1988;1:63.

26. Carroll EW, Wong-Riley MTT. Quantitative light and electron microscope microscopic analysis of cytochrome oxidase-rich zones in the striate cortex of the squirrel monkey. Journal of Comparative Neurology. 1984;222:1-17.

27. Carroll EW, Wong-Riley MTT. Correlation between cytochrome oxidase staining and the uptake and laminar distribution of tritiated aspartate, glutamate, gamma-aminobutyrate and glycine in the striate cortex of the squirrel monkey. Neuroscience. 1985;15:959-976.

28. Carroll EW, Wong-Riley MTT. Neuronal uptake and laminar distribution of tritiated aspartate, glutamate, gamma-aminobutyrate and glycine in the prestriate cortex of squirrel monkeys: correlation with levels of cytochrome oxidase activity and their uptake in area 17. Neuroscience. 1987;22:395-412.

29. Cartwright MJ, Anderson DR. Correlation of asymmetric damage with asymmetric intraocular pressure in normal-tension glaucoma (low-tension glaucoma). Arch Ophthalmol. 1988;106(7):898-900.

30. Casagrande VA, Kaas JH. The afferent, intrinsic, and efferent connections of primary visual cortex in primates. In Cerebral cortex vol 10. Ed: Alan Peters and Kathleen Rockland. Plenum Press, New York. 1994.

31. Chandler PA, Grant WM: Glaucoma. 2nd edition Philadelphia Lea and Febiger 1977.

32. Chandler, Grant. Glaucoma 4th edition Chapter 19 p199-211. Epstein DL, Allingham R, Schman J eds. Williams and Watkins 1997 Baltimore, Maryland.

33. Chaturedi N, Hedley-Whyte ET, Dreyer EB. Lateral geniculate nucleus in glaucoma. American Journal of Ophthalmology. 1993;116:182-188.

34. Chauhan BC, Drance SM. The relationship between intraocular pressure and visual field progression in glaucoma. Graefes Arch Clin Exp Ophthalmol. 1992;230(6):521-6.

35. Chong MS, Reynold ML, Irwin N, Coggeshall RE, Emson PC, Benowitz LI, Woolf CJ. GAP-43 expression in primary sensory neurons following central axotomy. J Neurosci 1994;310:316-336.

36. Cimler BM, Grebelhaus DH, Wakim BT, Storm DR, Moon RT. Characterization of murine cDNAs encoding P-57, a neural-specific calmodulin-binding protein. J Biol Chem. 1987;262:12158-12163.

37. Congdon N, Wang F, Tielsch JM. Issues in the epidemiology and population-based screening of primary angle-closure glaucoma. Surv Ophthalmol. 1992;36(6):411-423.

38. Cowey P, Stoerig A. Blindsight: neurons and behaviour. Prog Brain Res. 1993;95:445-459.

39. Crawford MLJ, Harwerth RS, Smith EL, Mills S, Ewing B. Experimental glaucoma in primates: changes in cytochrome oxidase blobs in VI cortex. Invest Ophthalmol Vis Sci 2001;42:358-364.

40. Crichton A, Drance SM, Douglas GR, Schulzer M. Unequal intraocular pressure and its relation to asymmetric visual field defects in low-tension glaucoma. Ophthalmology. 1989;96(9):1312-1314.

41. Dacey D, Peterson MR. Dendritic field size and morphology of midget and parasol ganglion cells in the human retina. Proc Natl Acad Sci. 1992;89:9666-9670.

42. Dandona L, Hendrickson A, Quigley HA. Selective effects of experimental glaucoma on axonal transport by retinal ganglion cells to the dorsal lateral geniculate nucleus. Investigative Ophthalmology and Visual Science. 1991;32(5):1593-1599.

43. Daniel PM, Whitteridge D. The representation of the visual field on the cerebral cortex in monkeys. Journal of Physioloy. 1961;159:203-221.

44. Darian-Smith C, Gilbert CD. Axonal sprouting accompanies functional reorganization in adult cat striate cortex. Nature. 1994;368(6473):737-740.

45. Darian-Smith C, Gilbert CD. Topographic reorganization in the striate cortex of the adult cat and monkey is cortically mediated.J Neurosci. 1995;15:1631-1647.

46. David R, Zangwill LM, Tessler Z, Yassur Y. The correlation between intraocular pressure and refractive status. Arch Ophthalmol. 1985;103(12):1812-1815

47. De La Monte SM, Federoff HJ, Ng SC, Grabcyk E, Fishman MC. GAP-43 gene expression during development: persistence in a distinctive set of neurons in the mature central nervous system. Dev Brain Res. 1989;46:161-168.

48. Diamond IT, Conley M, Itoh K, Fitzpatrick D. Laminar organization of geniculocortical projections in Galago senegalensis and Aotus trivirgatus. J Comp Neurol. 1985;22;242(4):584-610.

49. DiFiglia M, Roberts RC, Benowitz LI. Immunoreactive GAP-43 in the neuropil of adult rat neostriatum: localization in unmyelinated fibers, axon terminals and dendritic spines. J Comp Neurol. 1990;302:992-1001.

50. Ding Y, Casagrande VA. The distribution and morphology of LGN K pathway axons within the layers and CO blobs of owl monkey V1. Vis Neurosci. 1997;14(4):691-704.

51. Doster SK, Lozano AM, Aguayo AJ, Willard MB. Expression of the growth-associated protein GAP-43 in adult rat retinal ganglion cells following axon injury. Neuron. 1991;6:635-647.

52. Dreyer EB, Zurakowski D, Schumer RA, Podos SM, Lipton SA. Elevated glutamate levels in the vitreous body of humans and monkeys with glaucoma. Arch Ophthalmol.

1996;114(3):299-305.

53. Emery JM, Landis D, Paton D, Boniuk M, Craig JM. The lamina cribrosa in normal and glaucomatous human eyes. Trans Am Acad Ophthalmol Otolaryngol. 1974;78(2):290-297

54. Finkelstein I, Trope GE, Basu PK, Hasany SM, Hunter WS. Quantitative analysis of collagen content and amino acids in trabecular meshwork. Br J Ophthalmol. 1990;74(5):280-282.

55. Fitzpatrick D, Itoh K, Diamond IT. The laminar organization of the lateral geniculate body and the striate cortex in the squirrel monkey (Saimiri sciureus). J Neurosci. 1983 ;3(4):673-702.

56. Fitzpatrick D, Lund JS, Blasel GG. Intrinsic connections of macaque striate cortex. Afferent and efferent connections of lamina 4C. J Neurosci. 1985;5:3329-3349.

57. Fitzpatrick D, Lund JS, Schmechel DE, Towles AC. Distribution of GABAergic neurons and axon terminals in the macaque striate cortex. J Comp Neurol. 1987;264(1):73-91.

58. Gaasterland D, Tanishima T, Kuwabara T. Axoplasmic flow during chronic experimental glaucoma. 1. Light and electron microscopic studies of the monkey optic nervehead during development of glaucomatous cupping. Invest Ophthalmol Vis Sci. 1978;17(9):838-846.

59. Gaasterland D, Kupfer C. Experimental glaucoma in the rhesus monkey. Investigative Ophthalmology. 1974;13(6):455-457.

60. Gilbert CD, Wiesel TN. Receptive fields dynamics in adult primary visual cortex. Nature. 1992;356:150-152.

61. Glovinsky Y, Quigley HA, Dunkelberger GR. Retinal ganglion cell loss is size dependent in experimental glaucoma. Invest Ophthalmol Vis Sci.. 1991;32:484-490.

62. Glovinsky Y, Quigley HA, Pease ME. Foveal ganglion cell loss is size dependent in experimental glaucoma. Invest Ophthalmol Vis Sci.. 1993;34:395-400.

63. Gordon JA, Stryker MP. Experience-dependent plasticity of binocular responses in the primary visual cortex of the mouse. J Neurosci. 1996;16(10):3274-86.

64. Goslin K, Schreyer DJ, Skene JHP, Banker GA. Development of neuronal polarity: GAP-43 distinguishes axonal from dendritic growth cones. Nature. 1988;336:672-674.

65. Graham PA. Epidemiology of simple glaucoma and ocular hypertension. Br J Ophthalmol. 1972;56(3):223-229.

66. Harwerth RS, Carter-Dawson L, Shen F, Smith EL 3rd, Crawford ML. Ganglion cell losses underlying visual field defects from experimental glaucoma. Invest Ophthalmol Vis Sci 1999 40(10):2242-2250.

67. Haseltine EC, De Bruyn EJ, Cassagrande VA. Demonstration of ocular dominance columns in Nissl-stained sections of monkey visual cortex following enucleation. Brain Research. 1979;176:1153-158.

68. Hayreh SS. Pathogenesis of cupping of the optic disc. Br J Ophthalmol. 1974;58(10):863-876.

69. Heinen SJ, Skavenski AA. Recovery of visual responses in foveal V1 neurons following bilateral foveal lesions in adult monkey. Exp Brain Res. 1991;83(3):670-674.

70. Hendrickson AE, Wilson JR, Ogren MP. The neuroanatomical organization of pathways between the dorsal lateral geniculate nucleus and visual cortex in Old World and New world primats. J Comp Neurol. 1978;182:123-136.

71. Hendrickson AE, Hunt SP, Wu JL. Immunocytochemical localization of glutamic acid decarboxylase in monkey striate cortex. Nature. 1981;292:605-607.

72. Hendrickson AE, Tigges M. Enucleation demonstrates ocular dominance columns in Old World macaque but not New World squirrel monkey visual cortex. Brain Res. 1985;333:304-344.

73. Hendry SH. Delayed reduction in GABA and GAD immunoreactivity of neurons in the adult monkey dorsal lateral geniculate nucleus following monocular deprivation or enucleation. Exp Brain Res. 1991;86(1):47-59.

74. Hendry SHC, Fuchs J, deBlas AL, Jones EG. Distribution and plasticity of immunocytochemically localized GABA receptors in adult monkey visual cortex. J Neurosci. 1990;10:2438-2450.

75. Hendry SH, Jones EG. Reduction in number of immunostained GABAergic neurones in deprived-eye dominance columns of monkey area 17. Nature. 1986;320(6064):750-753.

76. Hendry SHC, Jones EG. Acitivty-dependent regulation of GABA expression in the visual cortex of adult monkeys. Neuron. 1988;1:701-712.

77. Hendry SHC, Kennedy MB. Immunoreactivity for a calmodulin-dependent protein kinase is selectively increased in macaque striate cortex after monocular deprivation. Proc Natl Acad Sci. USA. 1986;83:1536-1540.

78. Hendry SH, Yoshioka T. A neurochemically distinct third channel in the macaque dorsal lateral geniculate nucleus. Science. 1994;264(5158):575-7.

79. Hess DT, Edwards MA. Anatomical demonstration of ocular segregation in the retinogeniculocortical pathway of the New World capuchin monkey (Cebus apella). J Comp Neurol. 1987;264(3):409-20.

80. Hevner RF, Wong-Riley MTT. Regulation of cytochrome oxidase protein levels by functional activity in the macaque monkey visual system. J Neurosci. 1990;10(4):1331-1340.

81. Hiller R, Sperduto RD, Krueger DE. Race, iris pigmentation, and intraocular pressure. Am J Epidemiol. 1982;115(5):674-683.

82. Hoffman PN. Expression of GAP-43, a rapidly transported growth-associated protein, and class II beta tubulin, a slowly transported cytoskeletal protein, are coordinated in regenerating neurons. J Neurosci. 1989;9:893-897.

83. Horton JC. Cytochrome oxidase patches: A new cytoarchitectonic feature of monkey visual cortex. 1984;304:199-253.

84. Horton JC, Hedley-White ET. Mapping of cytochrome oxidase patches and ocular dominance columns in human visual cortex. Philosophical Transactions of the Royal Society B (London). 1984;304:255-272.

85. Horton JC, Hocking DR. Intrinsic variability of ocular dominance column periodicity in normal macaque monkeys. J Neurosci. 1996;16(22):7228-7239.

86. Horton JC, Hubel DH. Regular patchy distribution of cytochrome oxidase staining in primary visual cortex of macaque monkeys. Nature (Lond) 1981;292:762-764.

87. Hubel DH, Wiesel TN. Laminar and columnar distribution of geniculocortical fibers in macaque monkeys. J Comp Neurol. 1972;146:421-450.

88. Humphrey AL, Hendrickson AE. Background and stimulus-induced patterns of high metabolic activity in the visual cortex (area 17) of the squirrel and macaque monkey. J Neurosci. 1983;3(2):345-358.

89. Huntsman MM, Jones EG, Mohler H, Hendry SHC. Distribution of immunocytochemically localized GABA receptor subunits in monkey and human visual cortex. Soc Neurosci Abstr. 1991;17:115.

90. Jacobson M (ed) Handbook of Sensory Physiology Vol IX Development of Sensory Systems. Springer Berlin 1978 p55-83.

91. Jacobson RD, Virag I, Skene JH. A protein associated with axon growth, GAP-43, is widely distributed and developmentally regulated in rat CNS. J Neurosci. 1986;6(6):1843-1855.

92. Johnson JK, Casagrande VA. Prenatal development of axon outgrowth and connectivity in the ferret visual system. Vis Neurosci. 1993;10(1):117-30.

93. Johnson LV. Tonographic survey. Am J Ophthalmol. 1966;61:680-689.

94. Johnson JK, Casagrande VA. Distribution of calcium-binding proteins within the parallel visual pathways of a primate (Galago crassicaudatus). J Comp Neurol. 1995;356(2):238-260.

95. Johnston GAR, Allan RD, Skerritt JH. GABA receptors. In: Handbook of neurochemistry, vol 6. Lathja A ed. 1984. P213-237. New York: Plenum Press.

96. Jonas JB, Fernandez MC, Sturmer J. Pattern of glaucomatous neuroretinal rim loss. Ophthalmology. 1993;100(1):63-68.

97. Jonas JB, Gusek GC, Naumann GO. Optic disc morphometry in chronic primary open-angle glaucoma. I. Morphometric intrapapillary characteristics. Graefes Arch Clin Exp Ophthalmol. 1988;226(6):522-530.

98. Kanski J, McAllister JA, Salmon JF. Glaucoma: A colour manual of diagnosis and treatment 2nd edition. Butterworth Heinemann, Oxford, Boston. 1996.

99. Kanus P, Betz H, Rehm H. Expression of synaptophysin during postnatal development of the mouse brain. J Neurochem. 1986:47(4):1302-1304.

100. Karns IR, Ng SC, Freeman JA, Fishman MC. Cloning of complementary DNA for GAP-43, a neuronal growth-related proteins. Science. 1987;236:597-600.

101. Kaas JH, Krubitzer LA, Chino YM, Langston AL, Polley EH, Blair N. Reorganization of retinotopic cortical maps in adult mammals after lesions of the retina. Science. 1990;248(4952):229-31.

102. Kelly PT, McGuiness Tl, Greengard P. Evidence that the major postsynaptic density protein is a component of a Ca2+/calmodulin dependent protein kinase. Proc Natl Acad Sci USA. 1984;81:945-949.

103. Kennedy C, Des Rosiers M, Sokoloff L, Reivich M, Jehle J. The ocular dominance columns of the striate cortex as studied by the deoxyglucose method for measurement of local cerebral glucose utilization. Trans Am Neurol Assoc. 1975;100:74-77.

104. Kennedy MB, Bennett MK, Erondu NE. Biochemical and immunochemical evidence that the "major postsynaptic density protein" is a subunit of a calmodulin-dependent protein kinase. Proc Natl Acad Sci. 1983;80:7357-7361.

105. Kerrigan LA, Zack DJ, Quigley HA, Smith SD, Pease ME. TUNEL-positive ganglion cells in human primary open-angle glaucoma. Arch Ophthalmol. 1997;115(8):1031-1035.

106. Kirkwood A, Silva A, Bear MF. Age-dependent decrease of synaptic plasticity in the neocortex of a CAMKII mutant mice. Proc Natl Acad Sci USA. 1997;94:3380-3383.

107. Klein BE, Klein R. Intraocular pressure and cardiovascular risk variables. Arch Ophthalmol. 1981;99(5):837-839.

108. Krnjevic K. Some functional consequences of GABA uptake by brain cells. Neurosci Lett. 1984;47(3):283-287.

109. Lachica EA, Casagrande VA. Direct W-like geniculate projections to the cytochrome oxidase (CO) blobs in primate visual cortex: axon morphology. J Comp Neurol. 1992;319(1):141-158.

110. LeVay S, Connolly M, Houde J, Van Essen DC. The complete pattern of ocular dominance stripes in the striate cortex and visual field of the macaque monkey. J Neurosci. 1985;5(2):486-501.

111. LeVay S, Wiesel TN and Hubel DH. The development of ocular dominance columns in normal and visually deprived monkeys. J Comp Neurol. 1980;191:1-51.

112. Leventhal AG, Rodieck RW, Dreher B. Retinal ganglion cell classes in the Old World monkey: morphology and central projections. Science. 1981;213(4512):1139-1142.

113. Levy NS, Crapps EE. Displacement of optic nerve head in response to short-term intraocular pressure elevation in human eyes. Arch Ophthalmol. 1984;102(5):782-786.

114. Liang F, Jones EG. Differential and time-dependent changes in gene expression for type II calcium/calmodulin-dependent protein kinase, 67 kDa glutamic acid decarboxylase, and glutamate receptor subunits in tetanus toxin-induced focal epilepsy. J Neurosci. 1997;17(6):2168-2180.

115. Linda H, Piehl F, Dagerlind A, Verge VMK, Arvidsson U, Chullheim S, Risling M, Ulfhake B, Hokfelt T. Expression of GAP-43 mRNA in the adult mammalian spinal cord under normal conditions and after different types of lesions with special reference to motoneurons. Exp Brain Res. 1992;941:284-295.

116. Liu S, Wong-Riley M. Quantitative light- and electron-microscopic analysis of cytochrome-oxidase distribution in neurons of the lateral geniculate nucleus of the adult monkey. Vis Neurosci. 1990 Mar;4(3):269-287.

117. Liu XB, Jones EG. Localization of alpha type II calcium calmodulin-dependent protein kinase at glutamatergic but not gamma-aminobutyric acid (GABAergic) synapses in thalamus and cerebral cortex. Proc Natl Acad Sci U S A. 1996;93(14):7332-7336.

118. Livingstone MS, Hubel DH. Anatomy and physiology of a color system in the primate visual system. J Neurosci. 1984;4:309-356.

119. Livingstone MS, Hubel DH. Segregation of form, color, movement, and depth: anatomy, physiology, and perception. Science. 1988;240(4853):740-749.

120. Livingstone MS, Hubel DH. Thalamic inputs to cytochrome oxidase-rich regions in monkey visual cortex. Proc Natl Acad Sci U S A. 1982;79:6098-6101.

121. Livingstone MS. Hubel DH. Specificity of cortico-cortical connections in monkey visual system. Nature. 1983;304(5926):531-534.

122. Llinas R, McGuinness TL, Leonard CS, Sugimori M, Greengard P. Intraterminal injection of synapsin I or calcium/calmodulin-dependent protein kinase II alters neurotransmitter release at the squid giant synapse. Proc Natl Acad Sci U S A. 1985;82(9):3035-3039.

123. Malenka RC, Kauer JA, Perkel DJ, Mauk MD, Kelly PT, Micoll RA, Waxham MN. An essential role for postsynaptic calmodulin and protein kinase activity in long-term potentiation. Nature. 1989;340(6234):554-557.

124. Masliah E, Fagan AM, Terry RD, DeTeresa R, Mallory M, Gage FH. Reactive synaptogenesis assessed by synaptophysin immunoreactivity is associated with GAP-43 in the dentate gyrus of the adult rat. Exp Neurobiol. 1991:131-142.

125. Matthews MR, Cowan WM, Powell TPS. Transneuronal cell degeneration in the lateral geniculate nucleus of the macaque monkey. Journal of Anatomy. 1960;94:145-169

126. McGuinness TL, Brady ST, Gruner JA, Sugimori M, Llinas R, Greengard P. Phophorylation-dependent inhibition by synapsin I of organelle movement in squid axoplasm. J Neurosci. 1989;9:4138-4149.

127. McNeill TH, Mori N, Cheng HW. Differential regulation of the growth-associated proteins, GAP-43 and SCG-10 in response to unilateral cortical ablation in adult rats. Neuroscience 1999;90:1349-1360.

128. Meiri KF, Pfenninger KH, Willard MB. Growth-associated protein, GAP-43, a polypeptide that is induced when neurons extend axons, is a component of growth cones and corresponds to pp46, a major polypeptide of a subcellular fraction enriched in growth cones. Proc Natl Acad Sci. 1986;83:3537-3541.

129. Miller SG, Kennedy MB. Distinct forebrain and cerebellar isozymes of type II Ca2+/calmodulin-dependent protein kinase associate differently with the postsynaptic density fraction. J Biol Chem. 1985 Jul 25;260(15):9039-46.

130. Minckler DS, Bunt AH, Johanson GW. Orthograde and retrograde axoplasmic transport during acute ocular hypertension in the monkey. Invest Ophthalmol Vis Sci. 1977;16(5):426-41.

131. Minckler DS, Bunt AH, Klock IB. Radioautographic and cytochemical ultrastructural studies of axoplasmic transport in the monkey optic nerve head. Invest Ophthalmol Vis Sci. 1978;17(1):33-50.

132. Minckler DS. The organization of nerve fiber bundles in the primate optic nerve head. Arch Ophthalmol. 1980;98(9):1630-1636.

133. Mitchell DM and Timney B. Postnatal development of function in the mammalian visual system. In JM Brookhart, VB Mountcastle, I Darian Smith and SR Geiger (Eds), Handbook of physiology, section I. The nervous system, Vol III. Sensory processes, part I, Physiological society, Bethesda, MD, 1984, p507-555.

134. Mjaatvedt AE, Wong-Riley MTT. Relationship between synaptogenesis and cytochrome oxidase activity in Purkinje cells of the developing rat cerebellum. J Comp Neurol. 1988;277(2):155-182.

135. Morgan JE. Optic nerve head structure in glaucoma: astrocytes as mediators of axonal damage. Eye 2000a; 14 (Pt 3b):437-444.

136. Morgan JE, Uchida H, Caprioli J. Retinal ganglion cell death in experimental glaucoma. Br J Ophthalmology 2000b;84(3):303-310.

137. Murray KD, Gall CM, Benson DL, Jones EG, Isackson PJ. Decreased expression of the alpha subunit of Ca2+/ calmodulin-dependent protein kinase type II mRNA in the adult rat CNS following recurrent limbic seizures. Brain Res Mol Brain Res. 1995;32(2):221-232.

138. Nelson RB, Friedman DP, O'Neill Mishkin M, Routtenberg A. Gradients of protein kinase C substrate phosphorylation in primate visual system peak in visual memory storage areas. Brain Res. 1987;416(2):387-392.

139. Neve RL, Perrone-Bizzozero NI, Finklestein S, Zwiers H, Bird E, Kurnit DM, Benowitz LI. The neuronal growth-associated protein GAP-43 (B-50, F1): neuronal specificity, developmental regulation and regional distribution of the human and rat mRNAs. Brain Res. 1987;388(2):177-183.

140. Ng SC, De La Monte S, Conboy GL, Karns LB, Fishman MC. Cloning of Human GAP-43:growth association and ischemic resurgence. Neuron. 1988;1:133-139.

141. Nickells RW. Retinal ganglion cell death in glaucoma: the how, the why, and the maybe. J Glaucoma. 1996;5(5):345-356.

142. O'Brien C, Schwartz B, Takamoto T, Wu DC. Intraocular pressure and the rate of visual field loss in chronic open-angle glaucoma. Am J Ophthalmol. 1991;111(4):491-500.

143. Ouimet CC, McGuinness TL, Greengard P. Immunocytochemical localization of calcium/calmodulin-dependent protein kinase II in rat brain. Proc Natl Acad Sci U S A. 1984 Sep;81(17):5604-5608.

144. Perkins ES. Hand-held applanation tonometer. Br J Ophthalmol. 1965;49(11):591-593.

145. Pollack IP. Chronic angle-closure glaucoma; diagnosis and treatment in patients with angles that appear open. Arch Ophthalmol. 1971;85(6):676-689.

146. Polyak. 1957. The Vertebrate Visual System. University of Chicago Press Chicago, Illinois. 1390.

147. Portney GL. Photogrammetric analysis of the three-dimensional geometry of normal and glaucomatous optic cups. Trans Am Acad Ophthalmol Otolaryngol. 1976;81(2):239-246.

148. Quigley HA. Open-angle glaucoma. New England Journal of Medicine. 1993;238:1097-1106.

149. Quigley HA. Number of people with glaucoma worldwide. Br J Ophthalmol. 1996;80:389-393.

150. Quigley HA, Addicks EM. Chronic experimental glaucoma in primates, II: effect of extended intraocular pressure elevation on optic nerve head and axonal transport. Invest Ophthalmol Vis Sci. 1980;19:137-152.

151. Quigley HA, Addicks EM. Regional differences in the structure of the lamina cribrosa and their relation to glaucomatous optic nerve damage. Arch Ophthalmol. 1981;99(1):137-143.

152. Quigley HA, Addicks EM, Green WR. Optic nerve damage in human glaucoma. III. Quantitative correlation of nerve fiber loss and visual field defect in glaucoma, ischemic neuropathy, papilledema, and toxic neuropathy. Arch Ophthalmol. 1982 Jan;100(1):135-46.

153. Quigley HA, Anderson DR. The dynamics and location of axonal transport blockade by acute intraocular pressure elevation in primate optic nerve. Investigative Ophthalmology. 1976;15:606-616.

154. Quigley HA, Dunkelberger GR, Green WR. Chronic human glaucoma causing selectively greater loss of large optic nerve fibers. Ophthalmology. 1988;95:357-363.

155. Quigley HA, Dunkelberger GR, Green WR. Retinal ganglion cell atrophy correlated with automated perimetry in human eyes with glaucoma. Am J Ophthalmol. 1989;107(5):453-464.

156. Quigley HA, Green WR. The histology of human glaucoma cupping and optic nerve damage: clinicopathologic correlation in 21 eyes. Ophthalmology. 1979;86(10):1803-1830.

157. Quigley HA, Hohman RM, Addicks EM, Green WR. Blood vessels of the glaucomatous optic disc in experimental primate and human eyes. Invest Ophthalmol Vis Sci. 1984;25(8):918-31.

158. Quigley HA, Nickells RW, Kerrigan LA, Pease ME, Thibault DJ, Zack DJ. Retinal ganglion cell death in experimental glaucoma and after axotomy occurs by apoptosis. Invest Ophthalmol Vis Sci. 1995;36:774-786.

159. Quigley HA, Pease ME. Change in the optic disc and nerve fiber layer estimated with the glaucoma-scope in monkey eyes. J Glaucoma. 1996;5(2):106-116.

160. Quigley HA, Sanchez RM, Dunkelberger GR, L'Hernault NL, Baginski TA. Chronic glaucoma selectively damages large optic nerve fibers. Invest Ophthalmol Vis Sci. 1987;28:913-920.

161. Radius RL. Anatomy of the optic nerve head and glaucomatous optic neuropathy. Surv Ophthalmol. 1987;32:35-44.

162. Radius RL, Anderson DR. The course of axons through the retina and optic nerve head. Arch Ophthalmol. 1979;97(6):1154-1158.

163. Radius RL, Maumenee AE, Green WR. Pit-like changes of the optic nerve head in open-angle glaucoma. Br J Ophthalmol. 1978;62(6):389-393.

164. Radius RL, Pederson JE. Laser-induced primate glauocoma: I. Histopathology. Archives of Ophthalmology. 1984;102:1693-1698.

165. Rakic P, Goldman-Rakic PS, Gallager D. Quantitative autoradiography of major neurotransmitter receptors in the monkey striate and extrastriate cortex. J Neurosci. 1988;8:3670-3690.

166. Rodieck RW, Binmoeller KF, Dineen J. Parasol and midget ganglion cells of the human retina. J Comp Neurol. 1985;233(1):115-132.

167. Schreyer DJ, Skene JHP. Fate of GAP-43 in ascending spinal axons of DRG neurons after peripheral nerve injury: delayed accumulation and correlation with regenerative potential. J Neurosci. 1991;11:3738-3751.

168. Schulman H. Phosphorylation of microtubule-associated proteins by a Ca2+/calmodulin dependent protein kinase. J Cell Biol. 1984;99:11-9.

169. Schumer RA, Podos SM. The nerve of glaucoma. Arch Ophthalmol. 1994;112(1):37-44.

170. Segal P, Skwiercynska J. Mass screening of adults for glaucoma. Ophthalmologica. 1967;153(5):336-348.

171. Seligman AM, Karnovsky MJ, Wasserkrug HL, Hanker JS. Nondroplet ultrastructural demonstration of cytochrome oxidase activity with a polymerizing osmiophilic reagent, diaminobenzidine (DAB). Journal of cell biology 1968;38:1-14.

172. Shaw C, Cynader MC. Laminar distribution of receptors in monkey (Macaca fascicularis) geniculostriate systems. 1986;248:301-312.

173. Shields BM. Textbook of Glaucoma. Willliams and Wilkins, Baltimore, Maryland 1992:220-223.

174. Shin DH, Lee MK, Briggs KS, Kim C, Zeiter JH, McCarty B. Intraocular pressure-related pattern of optic disc cupping in adult glaucoma patients. Graefes Arch Clin Exp Ophthalmol. 1992;230(6):542-546.

175. Silva AJ, Stevens CF, Tonegawa S, Wang Y. Deficient hippocampal long-term potentiation in a-calcium-calmodulin kinase II mutant mice. Science. 1992;257:201-205.

176. Skene JHP, Jacobson RD, Snipes GJ, McGuire CB, Norden JJ, Freeman JA. A protein induced during nerve growth (GAP-43) is a major component of growth-cone membranes. Science. 1986;233:783-785.

177. Skene JHP, Willard M. Axonally transported proteins associated with axon growth in rabbit central and peripheral nervous systems. J Cell Biol. 1981a;89:96-103.

178. Skene JHP, Willard M. Changes in axonally transported proteins during axon regeneration in toad retinal ganglion cells. J Cell Biol. 1981b;89:86-95

179. Sommer A, Tielsch JM, Katz J, Quigley HA, Gottsch JD, Javitt JC, Martone JF, Royall RM, Witt KA, Ezrine S. Racial differences in the cause-specific prevalence of blindness in east Baltimore. N Engl J Med. 1991;325(20):1412-7.

180. Stone EM, Fingert JH, Alward WLM, Nguyen TD, Polansky JR, Sunden SLF, Nishimura D, Clark AF, Nystuern A, Nichols BE, Mackey DA, Ritch R, Kalenak JW, Craven ER, Sheffield VC. Identification of a gene that causes primary open angle glaucoma. Science. 1997;275(5300):668-70.

181. Sudhof TC, Lottspeich F, Greengard P, Mehl E, Jahn R. A synaptic vesicle protein with a novel cytoplasmic domain and four transmembrane regions. Science. 1987;238(4830):1142-1144.

182. Tetzlaff W, Alexander SW, Miller FD, Bisby MA. Response of facial and rubrospinal neurons to axotomy: changes in mRNA expression for cytoskeletal proteins and GAP-43. J Neurosci 11:2528-2544.

183. Tielsch JM, Katz J, Sommer A, Quigley HA, Javitt JC. Hypertension, perfusion pressure, and primary open-angle glaucoma. A population-based assessment. Arch Ophthalmol. 1995;113(2):216-221.

184. Tigges M, Hendrickson AE, Tigges J. Anatomical consequences of long-term monocular eyelid closure on lateral geniculate nucleus and striate cortex in squirrel monkey. J Comp Neurol. 1984;227(1):1-13.

185. Tighilet B, Hashikawa T, Jones EG. Cell- and lamina-specific expression and activity-dependent regulation of type II calcium/calmodulin-dependent protein kinase isoforms in monkey visual cortex. J Neurosci. 1998 Mar 15;18(6):2129-2146.

186. Tomlinson A, Philips CI. Applanation tension and axial length of the eyeball. Br J Ophthalmol. 1970;54(8):548-553.

187. Tootell RB, Hamilton SL, Silverman MS, Switkes E. Functional anatomy of macaque striate cortex. I. Ocular dominance, binocular interactions, and baseline conditions. J Neurosci. 1988;8(5):1500-1530.

188. Tootell RB, Silverman MS. Two methods for flat-mounting cortical tissue. J Neurosci Methods. 1985;15(3):177-190.

189. Trusk TC, Kaboord WS, Wong-Riley MTT. Effects of monocular enucleation, tetrodotoxin and lid suture on cytochrome-oxidase reactivity in supragranular puffs of adult macaque striate cortex. Visual Neuroscience. 1990;4:185-204.

190. Van Essen DC, Maunsell JHR. Two-dimensional maps of the cerebral cortex. J Comp Neurol. 1980;191:255-281.

191. Van Essen DC, Newsome WT, Maunsell JHR. The visual field representation in striate cortex of the macaque monkey: asymmetries, anisotropies and individual variability. Vision Research 1984;24(5):429-448

192. Van Hoff COM, Holthuis JCM, Oestreicher AB, Boonstra J, DeGraan PNE, Gispen WH. Nerve grwoth factor-induced changes in intracellular localization of the protein kinase C substrate B-50 in pheochromocytoma PC12 cells. J Cell Biol. 1989;108:1115-1125.

193. Varma R, Quigley HA, Pease ME. Changes in optic disk characteristics and the number of nerve fibers in experimental glaucoma. American Journal of Ophthalmology. 1992;114:554-559.

194. Vickers JC, Hof PR, Schumer RA, Wang RF, Podos SM, Morrison JH. Magnocellular and parvocellular visual pathways are both affected in a macaque monkey model of glaucoma. Australian and New Zealand Journal of Ophthalmology 1997;25:239-243.

195. Voigt T, De Lima AD, Beckmann M. Synaptophysin immunohistochemistry reveals inside-out pattern of early synaptogenesis in ferret cerebral cortex. J Comp Neurol. 1993;330(1):48-64.

196. Vulliet PR, Woodgett JR, Cohen P. Phosphorylation of tyrosine hydroxylase by calmodulin-dependent multiprotein kinase. J Biol Chem. 1984;259(22):13680-13683.

197. Walaas SI, Jahn R, Greengard P. Quantitation of nerve terminal populations: synaptic vesicle-associated proteins as markers for synaptic density in the rat neostriatum. Synapse. 1988;2(5):516-520.

198. Weber AJ, Kaufman PL, Hubbard WC. Morphology of single ganglion cells in the glaucomatous primate retina. Invest Ophthalmol Vis Sci. 1998;39:2304-2320.

199. Weber AJ, Chen H, Hubbard WC, Kaufman P. Experimental glaucoma and cell size, density and number in the primate lateral geniculate nucleus. Invest Ophthalmol Vis Sci. 2000;41(6)1370-1379.

200. Weber J, Koll W, Krieglstein GK. Intraocular pressure and visual field decay in chronic glaucoma. Ger J Ophthalmol. 1993;2(3):165-169.

201. Weber JT, Huerta MF, Kaas JH, Harting JK. The projections of the lateral geniculate nucleus of the squirrel monkey: studies of the interlaminar zones and the S layers. J Comp Neurol. 1983;213(2):135-145.

202. Wikstrom M, Krab K, Saraste M. Proton-translocating cytochrome complexes. Annu Rev Biochem. 1981;50:623-655.

203. Wong-Riley MTT. 1994 Primate visual cortex: Dynamic metabolic organization and plasticity revealed by cytochrome oxidase. Cerebral Cortex. Vol 10 Alan Peters and Edward Jones (eds). P141-200 Plenum Press, New York.

204. Wong Riley MTT. Cytochrome oxidase: An endogenous metabolic marker for neuronal activity. Trends In Neuroscience. 1989;12:94-101.

205. Wong-Riley M, Merzenich MM, Leake PA. Changes in endogenous enzymatic reactivity to DAB induced by neuronal inactivity. Brain Researc. 1978;141:185-192.

206. Wong-Riley M. Changes in the visual system of monocularly sutured or enucleated cats demonstrable with cytochrome oxidase histochemistry. Brain Research. 1979;171:11-28.

207. Wong-Riley M. Columnar cortico-cortical interconnections within the visual system of the squirrel and macaque monkeys. Brain Res. 1979;162(2):201-217.

208. Wong-Riley MTT, Carroll EW. Effect of impulse blockage on cytochrome oxidase activity in monkey visual system. Nature. 1984;307:262-264.

209. Wong-Riley MTT, Riley D. The effect of impulse blockage on cytochrome oxidase activity in the cat visual system. Brain research. 1983;261:185-193.

210. Wong-Riley MT, Tripathi SC, Trusk TC, Hoppe DA. Effect of retinal impulse blockage on cytochrome oxidase-rich zones in the macaque striate cortex: I. Quantitative electron-microscopic (EM) analysis of neurons. Vis Neurosci. 1989;2(5):483-497.

211. Wong-Riley MTT, Trusk T, Tripathi S, Hoppe D. Effect of retinal impulse blockage on cytochrome oxidase-rich zones in the macaque striate cortex, II: Quantitative EM analysis of neuropil. Vis Neurosci. 1989;2:499-514.

212. Yamaguchi T, Fugisawa H. Purification and characterization of the brain calmodulin-dependent protein kinase (kinase II), which is involved in the activation of tryptophan 5-monooxygenase. Eur J Biochem. 1983;132:15.

213. Yan DB, Coloma FM, Metheetrairut A, Trope GE, Heathcote JG, Ethier CR. Deformation of the lamina cribrosa by elevated intraocular pressure. Br J Ophthalmol. 1994;78(8):643-8.

214. Yoshioka T, Levitt JB, Lund JS. Independence and merger of thalamocortical channels within macaque monkey primary visual cortex: anatomy of interlaminar projections. Vis Neurosci. 1994;11(3):467-489.

215. Yucel YH, Gupta N, Kalichman MW, Mizisin AP, Hare W, de Souza Lima M, Zangwill L, Weinreb RN. Relationship of optic disc topography to optic nerve fiber number in glaucoma. Arch Ophthalmol. 1998;116(4):493-7.

216. Yucel YH, Kalichman MW, Mizisin AP, Powell HC, Weinreb RN. Histomorphometric analysis of optic nerve changes in experimental glaucoma. J Glaucoma. 1999;8(1):38-45.

217. Yucel YH, Zhang Q, Gupta N, Kaufman PL, Weinreb RN. Loss of neurons in magnocellular and parvocellular layers of the lateral geniculate nucleus in glaucoma. Arch Ophthalmol. 2000;118(3):378-384.

218. Zuber MX, Strittmatter SM, Fishman MC. A membrane-targeting signal in the amino terminus of the neuronal protein GAP-43. Nature. 1989;341:345-348.

Table 1: Animal Intraocular Pressure History history
Intraocular pressure (IOP) was measured in all animals and histology was performed on visual cortices. OD = right cortical hemisphere. OS = left cortical hemisphere. CO = cytochrome oxidase. GAP-43 = growth-associated protein 43. SYN = synaptophysin. GABA = GABAa receptor. CAMKIIα = calcium/calmodulin dependent protein kinase II α.

Table 1: Animal IOP History

Animal number		Period of Deprivation	Avg. Intraocular Pressure (mmHg)	Immunochemicals
91043	OD OS	2 months	39 ± 13 22 ± 3	CO, GAP, GABA: CO, SYN,
AI64	OD OS	2 months	50 ± 15 18 ± 3	CO, GAP, GABA: CO, SYN, CAMKIIa
K461	OD OS	4 months	49 ± 13 21 ± 8	CO, GAP, GABA: CO, SYN, CAMKIIa
AI15	OD OS	4 months	21 ± 3 41 ± 12	CO, GAP, GABA: CO, SYN, CAMKIIa
AI47	OD OS	4 months	37 ± 11 18 ± 3	CO, GAP, GABA: CO, SYN, CAMKIIa
94B083	OD OS	7 months	31 ± 14 18 ± 2	CO, GAP, GABA: CO, SYN, CAMKIIa
95B012	OD OS	7 months	17 ± 4 66 ± 21	CO, GAP, GABA: CO, SYN, CAMKIIa
1720	OD OS	Sham operated animal	20 ± 3 20 ± 3	CO, GAP, GABA: CO, SYN, CAMKIIa
410	OS	Normal	18 ± 7 22 ± 7	CO, GAP, GABA: CO, SYN, CAMKIIa
533	OD	Normal	16 ± 2 16 ± 4	CO, GAP, GABA: CO, SYN, CAMKIIa

Appendix

A. Types of glaucoma

i. Open angle glaucoma

Primary open angle glaucoma (POAG) or chronic open angle glaucoma (COAG) is the most common type of glaucoma seen by clinicians (Graham 1972). POAG is a slow progressive atrophy of the optic nerve, characterized by loss of peripheral visual function and optic disc cupping. It is associated with an IOP consistently above 21 mmHg; an open anterior chamber angle, a lack of ocular or systemic abnormality and visual field damage. In POAG, the angle of the anterior chamber can be wide or narrow, but it remains open under all conditions; therefore, the appearance of the angle in POAG patients is no different from normal individuals.

In the early stages of POAG, IOP is only slightly elevated, but it becomes progressively higher when the disease advances. Although the development of persistent IOP is a significant risk factor of glaucoma it is not a causative one because without the accompanying optic nerve head or visual field defect the patient may not develop glaucoma (Chauhan and Drance 1992; O'Brien, et al 1991; Weber et al, 1993,). POAG has been found to occur throughout a wide range of IOP (Sommer et al 1991) where patients who have low, or normal IOP can develop clinical symptoms of glaucoma and in contrast, patients with high levels of IOP may not necessarily develop the clinical symptoms (Graham et al 1972). Elevated IOP, ethnicity (it is most prevalent in individuals of African descent), vascular function, high refractive error, anatomic disorders and family history of glaucoma are all risk factors for human open angle glaucoma (Sommer et al 1991; Tielsch et al 1995).

Elevated IOP in POAG patients is caused by increased in resistance to aqueous outflow in the trabecular meshwork (Kanski 1996) (Figure 1). Various factors can influence the efficiency of outflow at the trabecular meshwork. Thickening, proliferation and orientation

changes in trabecular meshwork collagen, decrease in cellularity of the trabecular meshwork and thickening of the inter-trabecular spaces could all contribute to obstructing the outflow of aqueous humour (Alvarado et al 1984, Finkelstein et al 1990).

Elevated IOP causes damage to the optic nerve head which leads to topographic losses in visual fields (Quigley and Addicks 1981). The early stages of POAG is asympotmatic; therefore, visual field lost is not detected by the patient until significant damage has occurred in the optic nerve head. Topographically, central visual acuity remains normal until peripheral visual field loss is at an advanced stage. POAG typically affects both eyes and is believed to have a genetic basis. Recently, it has been found that a family history of glaucoma may be due to genes which code for the extracellular matrix molecule in aqueous outflow channels and this gene has been found to be associated with open angle glaucoma (Stone et al 1997).

ii. Closed angle glaucoma

Angle closure glaucoma occurs due to a partial or complete closure of the anterior chamber angle resulting in an obstruction of aqueous outflow (Figure 1). This type of glaucoma is often asymptomatic and occurs in eyes with shallow anterior chambers (Congdon, et al 1992). The most common form of angle closure glaucoma is the pupillary-block glaucoma in which there is a functional block between the pupillary portion of the iris and the anterior lens surface . In this type of glaucoma there is often a sudden increase in IOP.

Angle closure glaucoma can be acute, subacute or chronic. In acute angle closure glaucoma, the angle may suddenly close so that it is no longer functional. In this type of glaucoma, intermittent symptoms occurs before a sudden acute. When the portions of the anterior chamber is permanently closed and the IOP is chronically elevated, this is called chronic angle closure glaucoma (Bhargava et al 1973; Pollack 1971). In this condition, the symptoms are similar to those found in POAG.

iii. Normal tensive glaucoma

Normal tension glaucoma is characterized by glaucomatous optic disc damage and visual field loss with normal levels of IOP (Kanski 1996) Diagnosis for normal tensive glaucoma is often missed because the IOP is not elevated. It tends to affect central visual function earlier than POAG and is among the most difficult of glaucomas for physicians to manage (Chandler and Grant 1997).

Although normal tensive glaucoma has IOP levels within the normal range, its range is higher than those in the normal population. The small IOP increase has been found to be a slight causative factor in normal tension glaucoma (Araie et al 1994;Cartwright and Anderson 1988; Crichton et al 1989). Most patients with normal tensive glaucoma are asymptomatic and are diagnosed based on the optic nerve appearance.

iv. Congential glaucoma

Primary congenital open angle glaucoma is a specific inherited developmental defect of the trabecular meshwork and anterior chamber angle. In this type of glaucoma, the angle appears open. It is a significant cause of childhood blindness and the most common type of glaucoma in infants. Most investigators believe that the etiology of primary congenital glaucoma is caused by an obstruction at the trabecular meshwork (Shields 1992).